University of South-Eastern Norway

FMH606 Master's Thesis 2022
Process Technology

Minimum ignition energy of hydrogen and hydrogen-carrying fuels

Sarthak Jakar

Faculty of Technology, Natural sciences and Maritime Sciences
Campus Porsgrunn

Course: FMH606 Master's Thesis, 2022

Title: Minimum Ignition Energy of hydrogen and hydrogen-carrying fuels

Number of pages: 53

Keywords: MIE, Spark Energy, Hydrogen, Fuel – air equilibrium, Fuel – Oxygen equilibrium.

Student:	Sarthak Jakar
Supervisor:	Prof. Dag Bjerketvedt, Post Doc. Mathias Henriksen, Prof. Knut Vaagsaether
External partner:	MoZEES (www.mozees.no)

Summary: Hydrogen is touted to be the fuel of the future leading to low carbon emissions globally. But as this fuel is being popularized all over the world for all the industry sectors, very little is known about the combustion properties of hydrogen and its mixtures even though there has been a lot of research has been going on. Knowledge of its combustion properties will surely help in transportation, storage, and usage in different sectors. Therefore, the focus of this work is to determine the spark energy of the hydrogen-air mixture using a 20-liter explosion sphere ignition setup. The fuel mixture will be filled in the explosion sphere and the mixture will be ignited using a spark capacitance circuit by changing the capacitor as per the requirement for more energy. The data generated during the spark ignition is recorded on an oscilloscope and the visualization is done through Kirana, a high-speed camera that records the ignition inside the explosion sphere. Four experiments were performed under the 22_SJa_P01 and a total of 71 experiments under the 22_SJa_P02 project. The recorded data was then processed in MATLAB for which codes were developed to produce the plots for further analysis.

Preface

The experimental work done under this thesis was conducted at the Faculty of Technology, Natural Sciences, and Maritime Sciences at the University of South Eastern Norway campus Porsgrunn for the Master's course Process Technology. The tasks under this thesis assignment were given by Prof. Dag Bjerketvedt, Stip. Mathias Henriksen, and Prof. Knut Vagsaether. The external partner for this assignment was MoZEES which is a research center for developing zero-emissions technology systems.

And I thank everyone who has supported me throughout this thesis period directly or indirectly. I am grateful to have the opportunity to work under the guidance of Prof. Dag Bjerketvedt and thank him for the cooperation, encouragement, and insights on this topic and time investment throughout this period. Also, I want to show my gratitude to Post Doc. Mathias Henriksen for the valuable guidance under which all experiments were done, for helping through the development of the MATLAB codes, for helping in concept clarity, and for being supportive when some mistakes were committed. I also thank Associate Prof. Per Morten Hansen for providing the safety instruction at the start of lab work which helped in completing the laboratory task smoothly.

And finally, I value the moral and emotional support my friends and family in India provided me during this thesis and my elder brother's eye operation.

Porsgrunn, 17-05-2022

Sarthak Jakar

Contents

Nomenclature

H_2	Hydrogen
O_2	Oxygen
N_2	Nitrogen
CEM	Clean Energy Ministerial Hydrogen Initiative
IEA	International Energy Agency
MIE	Minimum Ignition Energy
USN	University of South-Eastern Norway
AC	Alternating current
DC	Direct current
K	Kilo
M	Mega
m	Milli
μ	Micro
n	Nano
P	Pico
F	Farad
Ω	Ohms
m	Meter
Hz	Hertz
V	Volt
W	watt

bar	Bar (pressure)
s	Seconds
λ	Air to fuel equivalent ratio
Φ	Fuel to air equivalent ratio
C	Capacitance

1 Introduction

This chapter will focus on the Objectives of this work, hydrogen as fuel of the future along with the challenges with hydrogen usage. This chapter will also cover the some international initiatives to counter the challenges with hydrogen usage.

1.1 Objectives

The objectives of this thesis report were to investigate the combustion properties of hydrogen and hydrogen-carrying fuels by developing a reliable and controllable spark ignition system for the facility that is USN using a 20-Liter explosion vessel to contribute to the clean energy transition. The approach for this is to perform a literature study on the minimum ignition energy of hydrogen and hydrogen-carrying fuels, to study a similar past experimental setup. Then Modelling the ignition system for the 20-Liter combustion vessel in Simulink, to which it was mutually agreed that it won't be a mandatory task. But still, an attempt has been made to contribute something to this task. And finally, Perform MIE experiments in the 20-Liter combustion vessel.

1.2 Motivation

Hydrogen now has been the buzzword in the field of energy in recent decades where both developing and developed countries are identifying its potential to be the fuel of the future. At present the major part of the world uses non-renewable sources to meet the energy demands in various sectors. This leads to not only carbon emissions but also other harmful elements leading to climate change. A study shows that steel industry alone contribute to 8% of the global emissions since as of now 1 tonne of coal-based steel produced accounts for about 1.5-3 tonne of carbon emissions as reported [1]. And even though if the use of hydrogen is adopted in some sectors, it's mostly in the grey hydrogen form which is produced through steam methane reforming. Therefore, a high demand for technological advancement are required to reduce the green hydrogen production cost to address global demand by 2030 [2]. Figure 1.1 shows the global demands by 2030 and Figure 1.2 shows the types of hydrogen, their souce and production method.
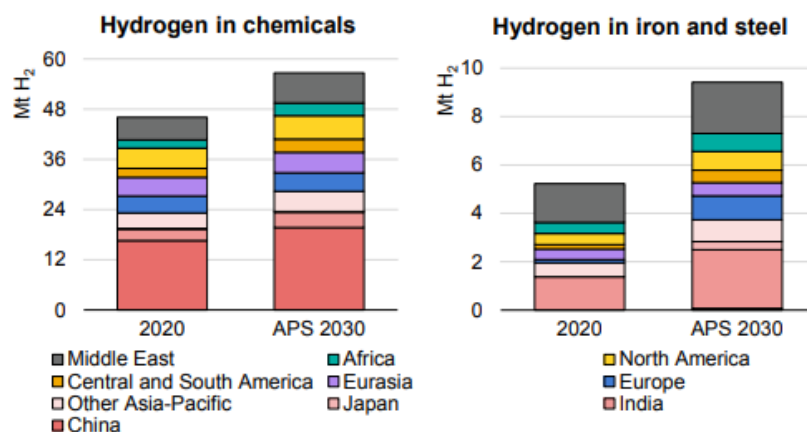

Figure 1.1: Global Hydrogen demand by 2030. [2]

Color	GREY HYDROGEN	BLUE HYDROGEN	TURQUOISE HYDROGEN*	GREEN HYDROGEN
Process	SMR or gasification	SMR or gasification with carbon capture (85-95%)	Pyrolysis	Electrolysis
Source	Methane or coal	Methane or coal	Methane	Renewable electricity

Note: SMR = steam methane reforming.
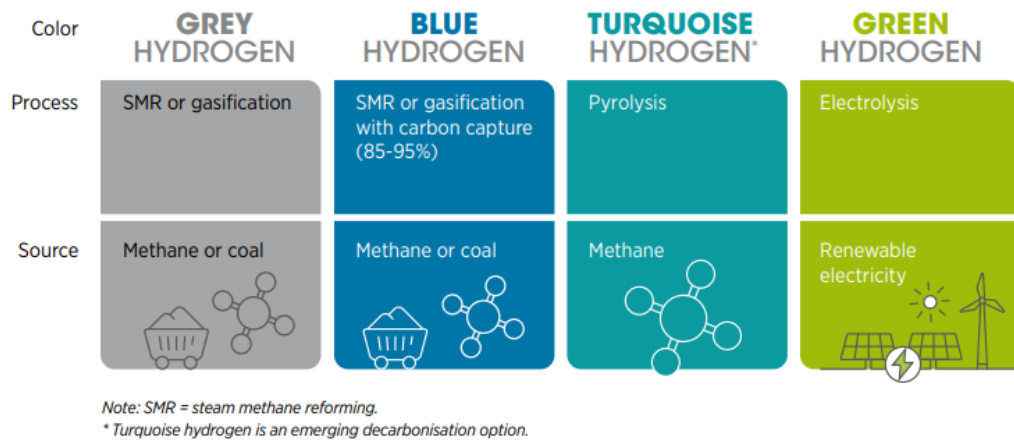* Turquoise hydrogen is an emerging decarbonisation option.

Figure 1.2: Shades of Hydrogen

Although the prospect of using hydrogen as the fuel of the future are expected to be high, it imposes a lot of issues such as safety, transportation, and storage as it requires about 3 times the more space than natural gases because of its low density. In a study Gexcon also laid out that hydrogen's flammability, buoyancy and ability to embrittle metals is a challenge [3]. Also several accidents have been reported all over the globe where uncontrolled ignition was the main cause of this tragedy like the one in Sandvika [4].

Global Initiatives such as the CEM hydrogen Initiative which stands for the Clean Energy Ministerial Hydrogen Initiative coordinated by the International Energy Agency (IEA) has bring about the governments of developed and developing nations together to put the role of hydrogen and the fuel cell technology under radar for global clean energy shift. CEM targets successful deployment of the hydrogen in different industrial sectors and meeting the energy need of the society [5]. To curb the carbon emissions through the steel industries, G7 countries are trying to eliminate 30% of the emissions by 2030 so to reach the zero carbon emissions in the steel industry by 2050 [1].

2 Theory on MIE

This chapter covers some theories behind the minimum ignition energy and also reflects the previous research done in the development of a more robust and reliable ignition testing apparatus.

2.1 MIE definition

Ignition Energy is an important characteristic to be understood when it comes to a fuel / gas mixture potentially thought to be replaced as a fuel for the future in industry since it becomes important to know at what smallest energy a substance mainly the gas mixture here will ignite. And therefore, this smallest energy required to ignite a gas/fuel mixture or a combustible material at a fixed pressure and temperature becomes the Minimum Ignition Energy at those concentrations.

Factors like fuel concentrations, type of oxidizer, temperature, pressure, and flow characteristics, ignition source affect this MIE value. More factors are discussed in chapter 3. Table 2.1 gives overview of MIE of some furl / air at stoichiometry.

Table 2.1: MIE of some furl / air at stoichiometry [6].

Sno.	Substance	MIE [mJ]	Sno.	Substance	MIE [mJ]
1	Hydrogen (H2)	0.017	4	Ethene (C2H4)	0.070
2	Methane (CH4)	0.028	5	Butane (C4H10)	0.25
3	Ethane (C2H6)	0.24	6	Ammonia (NH3)	680

This work used mainly two ways to calculate the capacitive spark energy which is the energy that was discharged from the charged capacitor to ignite the hydrogen – air mixture.

$$E_{spark} = \int |U(t) \cdot I(t)| dt \tag{2.1}$$

Equation 2.1 was used in the MATLAB scripts as the idea for the numerical integration of the scaled current and the voltage data obtained from the oscilloscope 2. Whereas the equation 2.2 was used to calculate the theoretical energy that can be expected from the test setup which directly is dependent on the capacitance used.

$$E = \frac{1}{2} CV^2 \tag{2.2}$$

Precious research work on Ignition System

2.1.1 Research and studies of B. Lewis and von Elbe.

The works laid out by B.Lewis and von Elbe are considered as the standard data in almost every modern research MIE research. Using their experimental setup, they calculated the MIE of propane air mixture was turned out to be 0.26 mJ at the ambient conditions [7]

Initially designed by Guest in 1944 and then later modified Blanc, Guest, von Elbe and Lewis in 1947 the test bomb made up of stainless steel had a diameter of 127 mm. For adjustment the gap length between the flanged electrodes a micrometer was attached to it.

The ignition through spark ignition was a found to be a risky process as concluded by K.G. Strid. It was concluded that capacitive sparks have high accidental chances, for example a large spark energy can be hazardous and can lead to uncontrolled ignition whereas a small ignition perhaps might even not ignite the mixture. Therefore, spark length as a major factor was considered as a point of focus in the studies by P.G. Guest and the experimental findings with this apparatus served as a basis for determine the minimum ignition energy [7]. There was one problem with setup used for determining the ignition energy, the flanged electrodes used were susceptible to corona discharge and which would lead to irregular discharges resulting in uncontrolled ignitions. to correct these glass flanges were used then eventually these were also coated with paraffin wax. In the end as suggested by Strid and Litchfield flanges were kept more conductive for uniform distribution of charge.

Figure 2.1 shows an apparatus capable of generating a spark with the capacitance of 100 pF or more. A high voltage input is given at terminal "a" which is then carried forward to terminal "b" and then to electrodes in test bomb when the rotary charger engages. The transfer of the high voltage is governed by the speed of the rotary charger. The test bomb is filled with the fuel mixture once the spark gap between the electrodes is set using the micrometer. In case if ignition is not successful a new capacitor can be used and the rotary charger can be replaced by the resistor rod. When higher capacitance is used, time delay is observed during the spark. To mitigate this radium capsules are used in the test bomb.
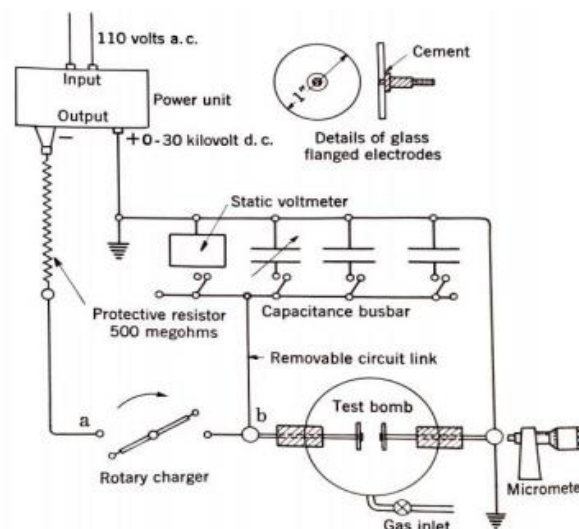

Figure 2.1: Setup for determining minimum ignition energy for electric-spark ignition [7]

If the capacitors used in the experiments are less than 100 pF, a modified model of the apparatus is prepared. Figure 2.2 shows such apparatus. Here the rotary charger is replaced by Bakelite rod which is in order of 10^{11} ohms. The static voltmeter and the capacitors are now connected in parallel instead of series as in previous setup and the power can be transferred to test bomb through the Bakelite rod. The order of capacitance can be adjusted as low as 1 pF with the help of the small rod and ball capacitors used.
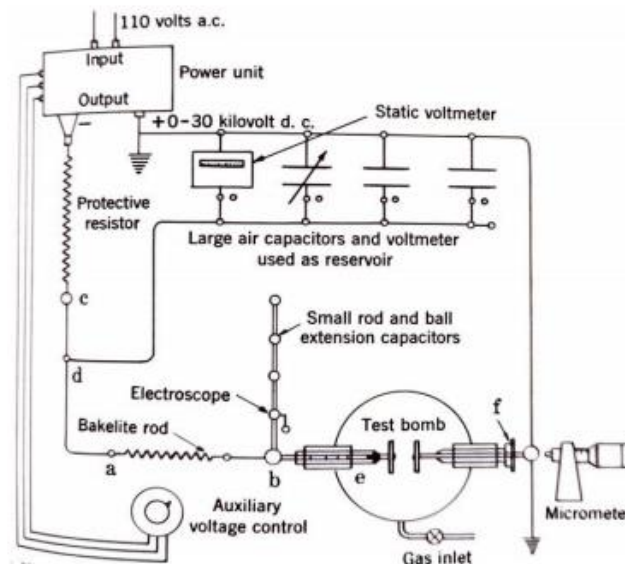

Figure 2.2: Apparatus arranged for spark circuits of very low capacitance [7]

2.1.2 Research by ASTM.

Another test method based on the works of Lewis and von Elbe and Bureau of mines was developed in year 2007 known as the ASTM method shown in figure 2.3. In this model the breakdown voltage of the spark is governed by the Paschen's law. The apparatus has reaction vessel of 1 dm^3 made of stainless steel. An isolating resistor is placed near the DC supply terminal with order of 10^{12} ohms. For the fuel mixtures which requires high spark energy to ignite, the value of the resistor is varied inversely as the capacitor value is increased. The test method uses capacitor in the range of 8-12 pF and the DC supply is in order of 1-30kV. The test method provides accuracy of $\pm$ 10% in calculations of minimum ignition energy.
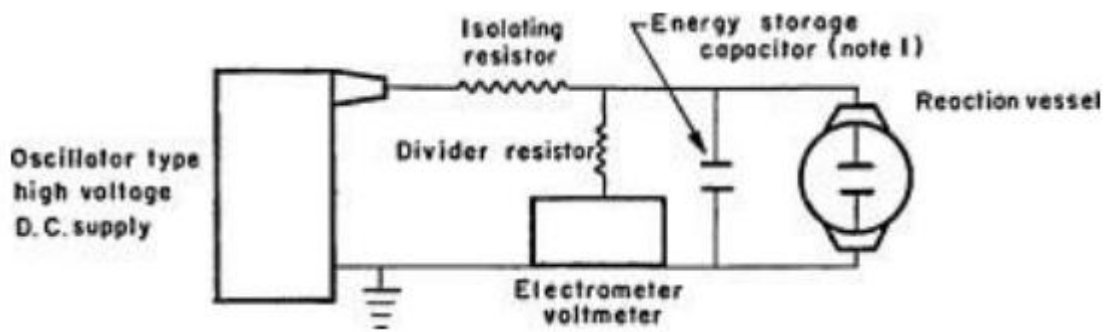
Figure 2.3: Electrical circuit from ASTM (2007) [8]

2.1.3 Research by Moorhouse et al.

Another test method or setup was designed by Moorhouse et al for determination of MIE for hydrocarbons/air mixtures shown in figure 2.4. [8] The test apparatus has stainless steel test vessel with diameter of 50 mm and length 200 mm. The capacitor consisted of two parallel plates of 100x200 mm in dimension. The capacitance used in this setup was in the range of 19-64 pF and the inductance and resistance of the external circuit was kept very low, 1μH and 2μΩ respectively. The outcome of this setup was quite interesting to see, it was found that the MIE decreased with increase in the unburnt mixture temperature and pressure. Also the MIE for the propane /air mixture at the normal / standard conditions of 5.3 vol % was 0.46 mJ, higher than what was founded by Lewis and von Elbe which was reported to be 0.25 mJ.
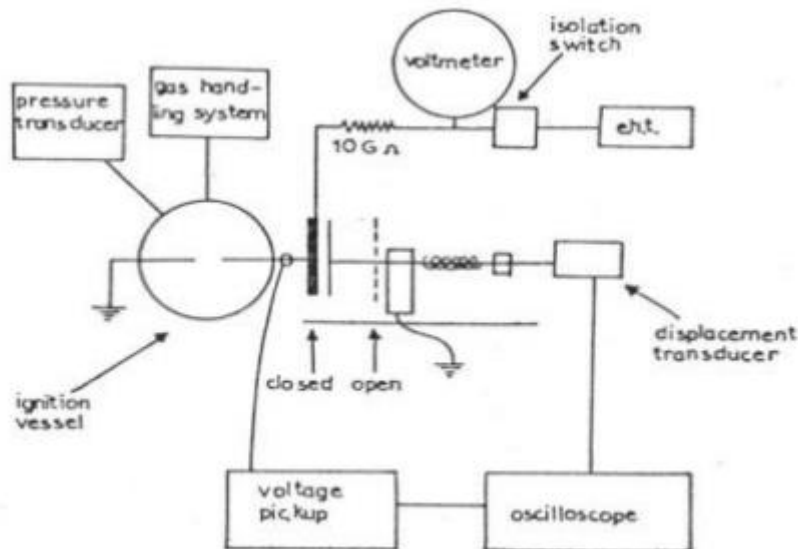

Figure 2.4: Electrical circuit from Moorhouse et al. (1974) [8]

2.1.4 Research by Randeberg et al.

A different setup shown in figure 2.5 was developed by Randerberg et al. which had a cylindrical explosion vessel with diameter of 11.5 cm and volume of 1.2 dm^3. Tungsten electrodes were used with diameter of 2.0 mm with gap width in range of 1.0 mm to 6.0 mm. the setup uses 1μF as a primary capacitor which is charged to 300 V. The capacitor then discharged in the primary coil induces a set up voltage of 15kV in the secondary coil. There is chance of recharging the capacitor in the primary coil, to avoid this time constant RC is set to be 1μs and R value is decided in the range of 100 kΩ to MΩ. [9]
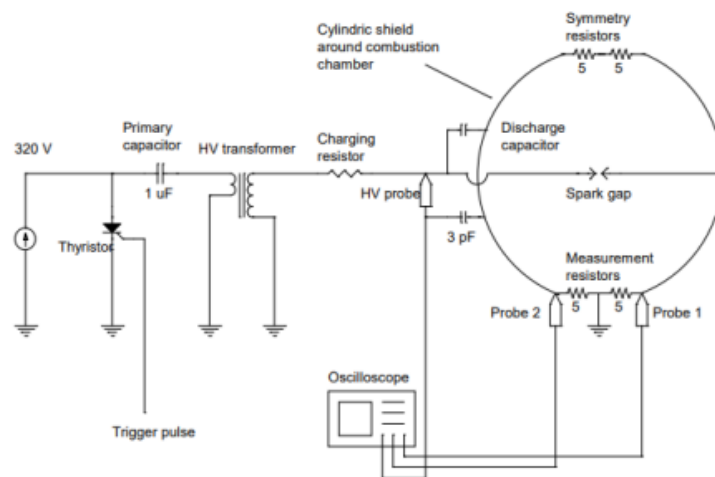
Figure 2.5: Electrical circuit from Randeberg et al. (2006) [9]

Figures 2.6 shows the spark energy results in comparison to the works by Kono et al [10] Moorhouse et al, Lewis von Elbe [9] indicating ignition or no ignition for 2 mm and 4 mm gap distance between electrodes. The differences found in the results for spark energy and the same concentration of the fuel used are subjected to the type of the experimental setup and factors discussed in the literature review.

Figure 2.6: Different MIE for ignition of propane-air mixtures, from Randeberg et al. (1974) [9]

3 Factors affecting the Ignition energy.

This chapter will cover the factors which directly affect the spark energy outcome when experiments are performed. Factors such as Humidity, spark duration, elevated temperature and pressure, electrode gap, electrode geometry and so on are discussed.
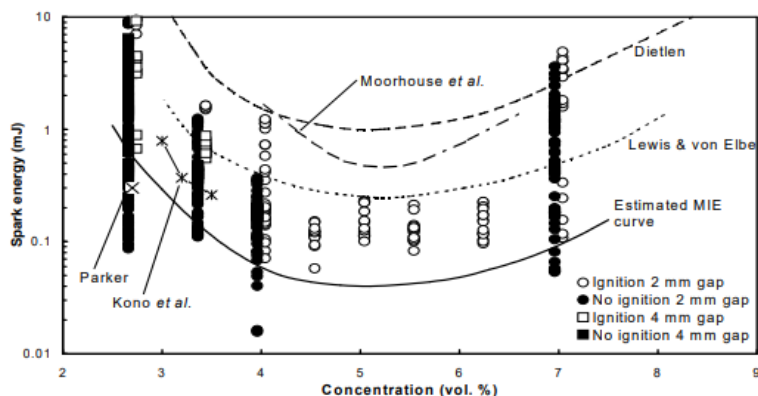
3.1 Humidity and spark duration.

Effects of humid environment on the minimum ignition energy of the hydrogen-air mixture were studied by R. Ono et al., by increasing the humidity from 0 to 90 % and the MIE was measured using a capacitive spark and an RC circuit in series. The results in figure 3.1 showed that there was only a slight increase in the MIE which indicated that increase in humidity had no significant effect on the MIE. Effect of the varied spark duration from the range of 5ns to 1ms were also investigated by R. Ono et al. and concluded that the MIE of H_2 – dry air mixture is approximately constant. The work by R.Ono et al also compare his work with all the previous works that have been done in determining the Minimum Ignition Energy of the H2 and its mixtures. It can be represented in the figure 3.2. [11]
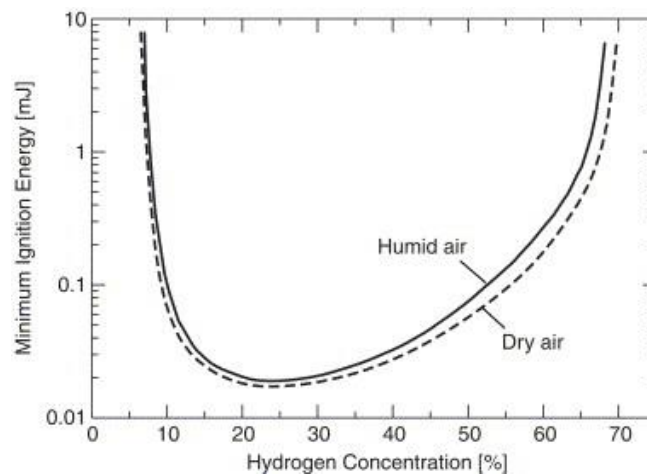

Figure 3.1 MIE of hydrogen-humid air and hydrogen-dry air mixtures [11]
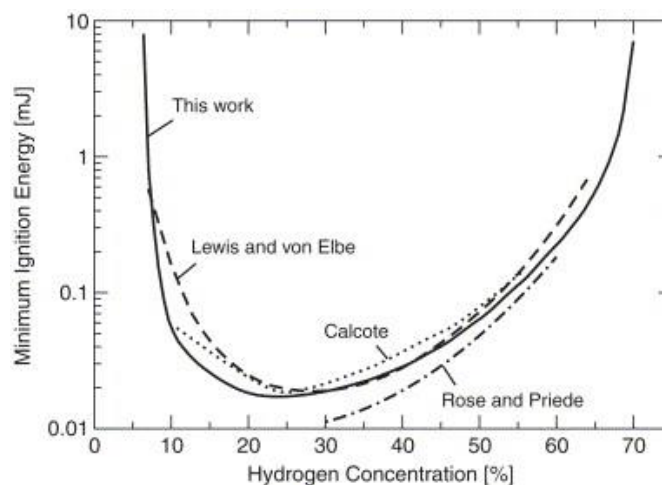

Figure 3.2: MIE of hydrogen–dry air mixture obtained in this work and previous studies [11]

3.2 Effect of Elevated temperatures and pressure.

Results obtained by Gan Cui at el. [12] Studied the effects of the elevated temperature pressure using their experimental setups and discovered that the MIE has a higher order linear relationship with pressure i.e $1/P^2$ and an approximately linear relationship with the temperature in the order of $1/T$. It was also concluded that with the increase in pressure, the influence of temperature on the MIE becomes insignificant and vice versa. Relation shown in figure 3.3

(a)   (b)
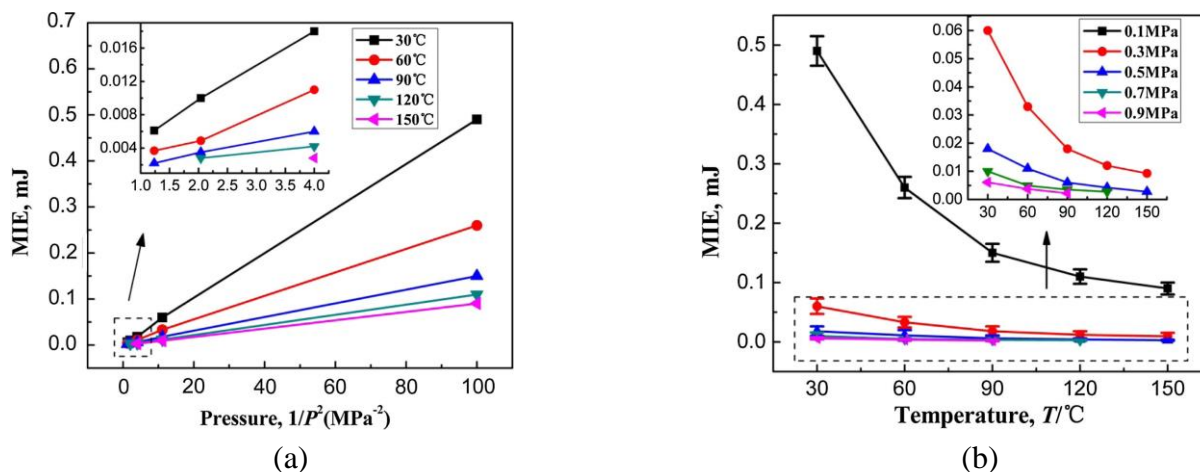
Figure 3.3: (a) Relation of MIE and pressure, (b) Relation of MIE and Temperature. [12]

3.3 Type of Ignition mechanism

For a fuel mixture to ignite, its important that the ignition source provides enough energy in the form of heat to the fuel mixture so that a sustained burning can be achieved. Since the ignition is an end product of a chemical reaction exothermic in nature, this can have different attributes to it depending on which type of source is used. Studies done on classification of ignition mechanism suitable for hydrogen and its mixture are listed in the table 3.1. Some of the methods are still debatable.

Table 3.1: Classification of Ignition sources [13]

Sno.	Type of Ignition	Attributes and Initiation
1	Adiabatic compression or turbulence	Ignition by Shock waves by compression through equipment geometry at the point of release.
2	Diffusion ignition	Ignition of 3:1 hydrogen nitrogen mixture at temperature 575 K, still below experimented auto ignition temperature hydrogen. It's debatable whether ignition will be caused by this method.
3	Hot-surface ignition	Mixture is exposed to surface having higher temperature than autoignition temperature.

4	Reverse Joule-Thompson effect	Temperature of hydrogen rises when depressurized, rather than fall. Rise in temperature usually never leads to temperature where hydrogen can auto ignite.
5	Electrostatic ignition	Ignition through sparks, brush discharges, corona discharge.

The experiments done in this work uses spark ignition mechanisms where capacitive sparks are generated between the electrodes. Electrical sparks are a result of breaking of low-voltage highcurrent circuits whereas the electrostatic sparks are a result of high-voltage low-current circuit when the electric field is high enough to lead to electrical breakdown in fuel mixture between electrodes [9] where the Spark energy is expressed same as equation 2.2.

$$E = \frac{1}{2}CV^2 \tag{3.1}$$

3.4 Electrode Gap

Paschen's Law is a equation which governs the breakdown voltage and breakdown voltage is a voltage value required to initiate a discharge the energy to the electrodes in a combustible mixture as a function of pressure and gap length. [14].

In 2020 J. Liu et al. did some experiments to understand the spark discharge and found out that the peak of the field intensity of the three electrodes used (2 mm, 4 mm, 6 mm) increases when it is closer to the electrode tip and the field intensity is inversely proportional to the gap length but directly proportional to the voltage shown in figure 3.4 (a). And with increasing gap length the spark resistance is greater as more ionization energy is required, as shown in figure 3.4 (b). [15]

(a)   (b)
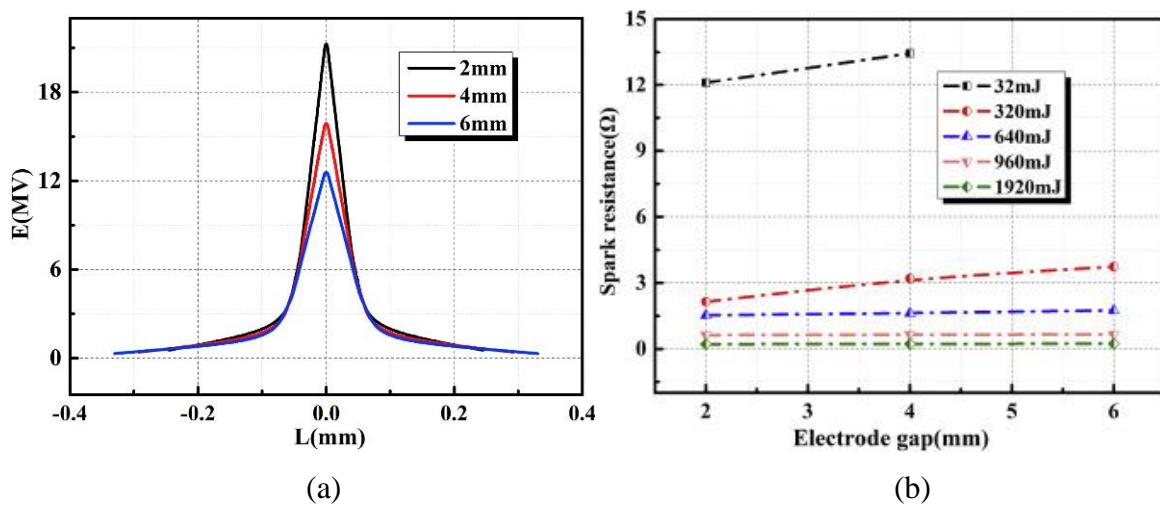
Figure 3.4: Effect of electrode gap on spark discharge: (a) Field intensity distribution on the electrode surface under different electrode gaps, (b) Variation of spark resistance with electrode gap. [15]

The Smithsonian table and the handbook of chemistry and physics records a study where the a correlation of the Electrope gap and geometry influencing the spark gap breakdown voltage can be observed. But is seen that for same electrode shape / geometry and gap length both records different spark gap breakdown voltage for air. Thus, it could said other factors might be responsible for such difference but it can also be concluded from figure 3.5 that increasing the gap length surely increases the required breakdown voltage. [16]
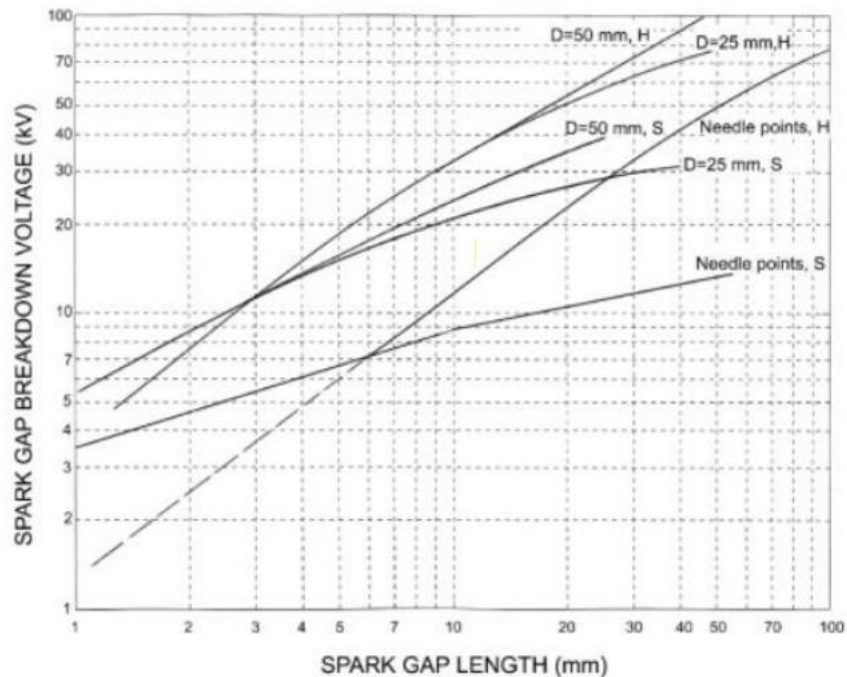
Figure 3.5: Spark gap breakdown voltages in air, where "H" is data from the Handbook of Chemistry and Physics and "S" is data from Smithsonian Physical Tables [16]

Since the gap length is one of the major factor deciding the MIE for the fuel mixtures along with dependency on the concentrations used, R. Ono et al provided study of MIE for hydrogen-dry air mixtures at different concentrations shown in figure 3.6 [11].

(a)	(b)
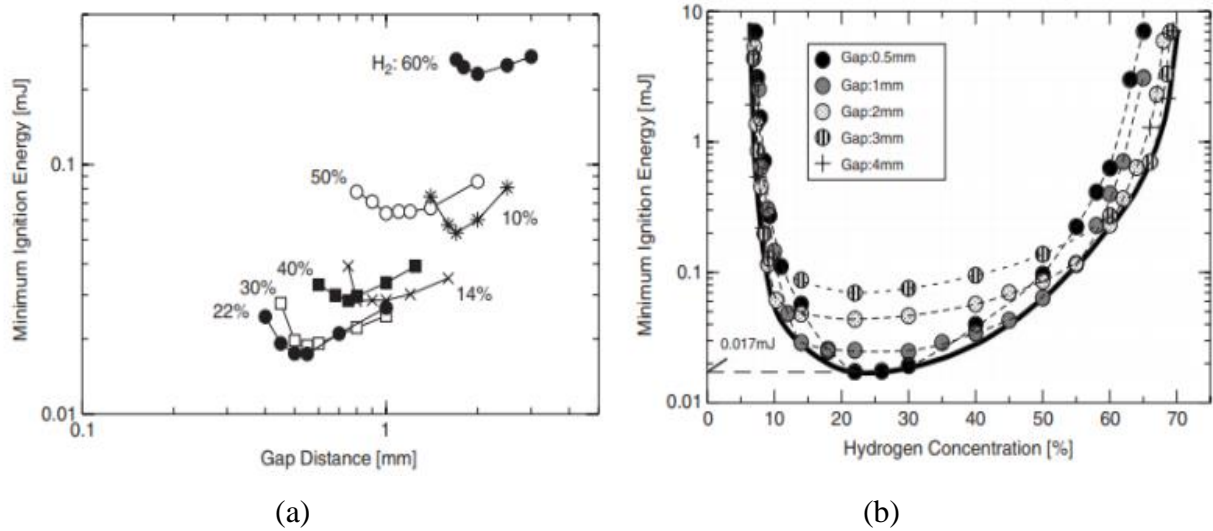
Figure 3.6: MIE of hydrogen-dry air mixture for different gap distance: (a) for increasing gap distance, (b) for fixed gap distance [11]

3.5 Effect of electrode geometry.

Sally P.M Bane et al in 2015 performed some ignition experiments [17] of the product of 15% hydrogen-air mixture with three electrodes namely cylindrical / wire, conical, and flanged, in order to investigate the effect of electrode geometry on the flow field and flame formation. Ignition were captured via the schlieren visualization, and the computational simulations were done for the same. Figure 3.7 (a) shows the results of the simulation and experimental setup for cylindrical electrode and figure 3.7 (b) shows the results of the simulation and experimental setup for the conical electrode. It was found that flow field for both geometries was quite similar leading to similar flame formation. The flame front develops in two parts, its initiated on the boundary of the vortex and then the outside of hot gas kernel which is influenced by the successive vortex.
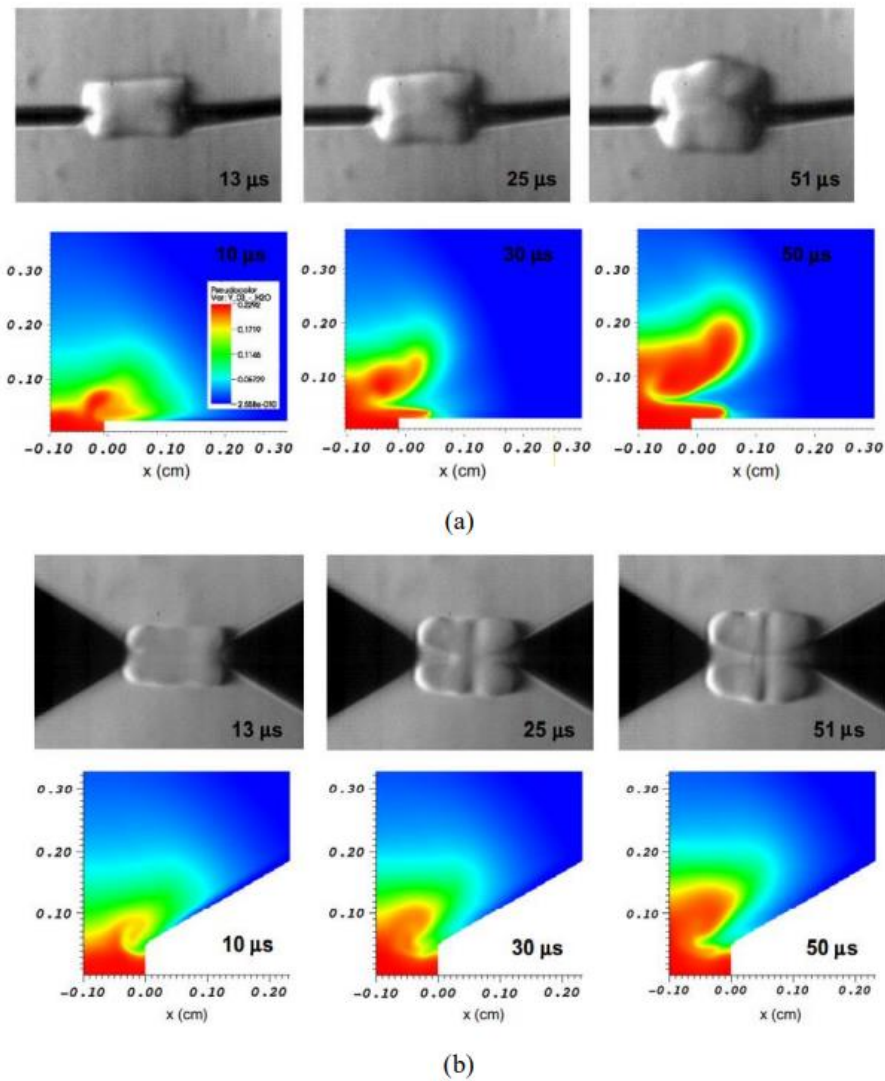
Figure 3.7 : Images from high-speed schlieren visualization and simulation of ignition: (a) for cylindrical electrodes, (b) for conical electrodes [17]

Figure 3.8 shows the experimental and simulation result of the flanged electrode respectively, where both the experimental and simulation results indicate the for flanged electrode viscous effect leads to multi-dimensional flow. In flanged electrodes viscous effect generated vortices which trap the hot mixture kernel are quite similar to that of conical and cylindrical electrodes but the flange in the geometry leads but entrapment of hot mixture kernel resulting in lower ignition energy and lower time delays.
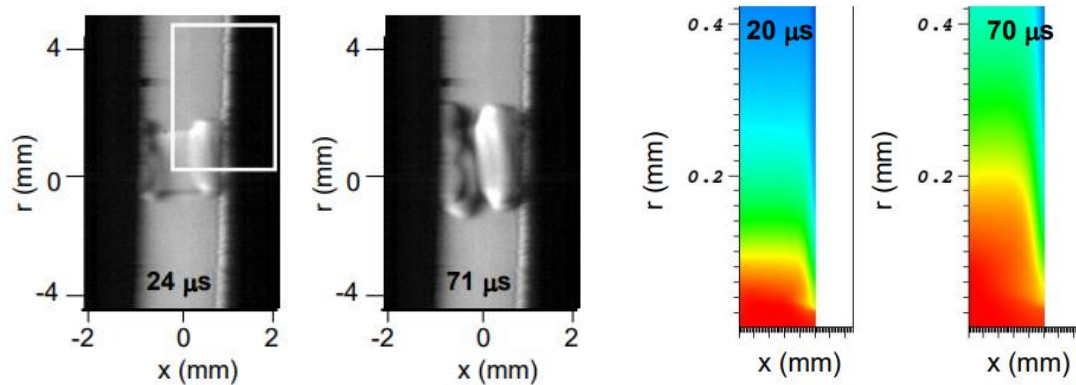
Figure 3.8: Images from high-speed schlieren visualization and simulation of ignition for flanged electrodes [17]

3.6 Statistical MIE

A study to determine the MIE through statistical approach was done by Wahner et al [18]where a experimental setup was prepared showed in figure 3.9 and test were conducted for hydrogen. Logistic regression was used to characterize the statistical pattern of the experimental data and MIE along with Ignition probability were determined. The hydrogen concentration was 22.0 % and the electrodes had a varied length between 0.40 mm to 0.75 mm and the capacitance in range of 3.6 pF to 10.4 pF. The values determined are stated in the form "measured value ± expanded value uncertainty", to not neglect the measurement uncertainty of capacitance and voltage, where at least 0.5 pF uncertainty for capacitance was considered. This resulted MIE based on the resulted as (17.2 ± 2.3 μJ).
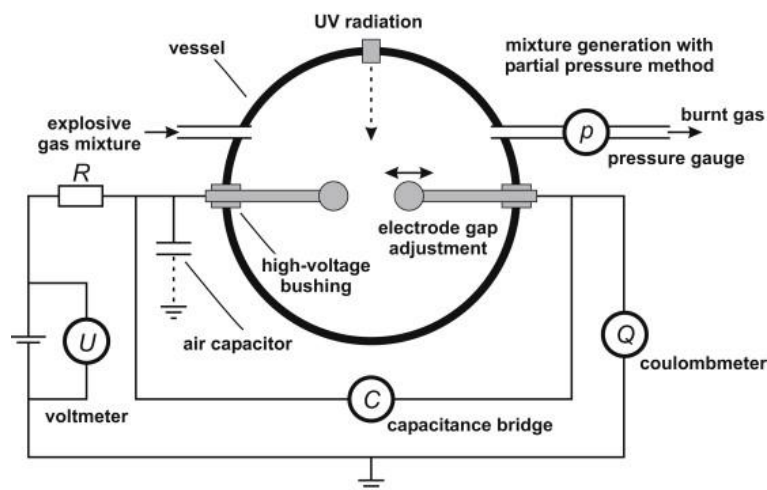
Figure 3.9. Experimental setup by Wahner et al. [18]

Figure 3.10 (a) shows the Ignition energy determined in the experiments in compared to the MIE value found by Brandes and Moller in 2008. For the ignition probability Fromm in 2010 laid out few conditions which apply to the logistic regression [18]. The outcome of the logistic regression is the function described in equation 3.2 where β_0 is constant regression parameter, β_1 is the influence of the independent variable X on the probability slope :

$$P(x) = \frac{1}{1 + \exp(-\beta_0 - \beta_1 \cdot x)} \tag{3.2}$$

For hydrogen, the probability curve shown in figure 3.10 (b) is expressed by equation 3.3. And upon calculations the tabulated MIE and MIE from experiments had ignition probability of 0.85% and 0.97 %, respectively.

$$P(x) = \frac{1}{1 + \exp(11.919 - 0.422 \cdot x)} \tag{3.3}$$

(a)   (b)
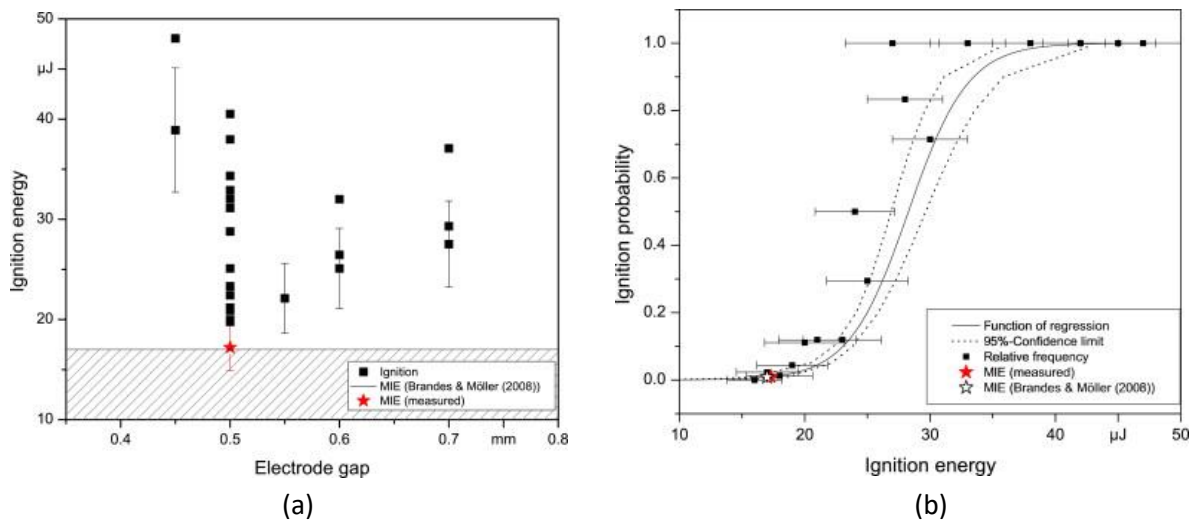
Figure 3.10 : (a) Ignition energy of Hydrogen, (b) Ignition Probability [18]

4 Experimental setup.

The experimental work presented in this thesis is based on lab experiments performed at the USN laboratory. A capacitance electrical circuit was used to generate the spark ignition through electrodes inside the explosion sphere. This chapter will focus describing the experimental setup, equipment used while performing the experiments.

4.1 Ignition system.

A capacitive spark ignition circuit is used in this lab setup where a high-power supply XP EMCO model Q101-5 is used as an ignitor. A representation of the spark ignition circuit available at the USN laboratory is represented in figure 4.1. The connection leads made of tinned copper clad steel are used to connect the circuit. In principle, when the capacitor is charged to the supplied voltage it does not dissipate the energy, therefore it's made to discharge the stored energy to the electrodes gap also called spark gap which is connected in parallel arrangement to the capacitor which then forms an energy spark at the gap breakdown voltage. To achieve ignition for the hydrogen mixture concentration where the lambda is low, a higher order capacitor for example. 20nF can be used by swapping out or combining it with the other capacitors.

Figure 4.1: Capacitor Ignition Circuit.

Another type of circuit used in this kind of experiments are RC circuit which stands for resistor-capacitor circuit which is shown in figure 4.2 (b). For all the 22_SJa_P102 experiments a capacitive circuit is used shown in figure 4.2 (a).
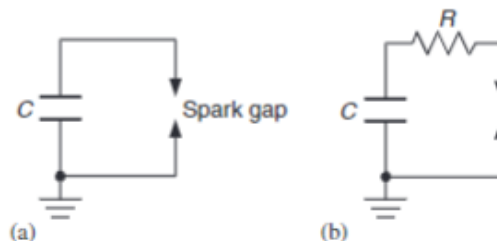
Figure 4.2: (a) Capacitance circuit, (b) RC circuit.

Figure 4.3 displays a pulse generator with multiple channels used to control the high voltage power supply. Model specification of the pulse generator is Quantum 9518 which has input of 12V and can handle pulse frequency equal to 5MHz with impudence of about 40pF. It is very important to check the channel interface on the display of the pulse generator along with the charging time provided in milliseconds.
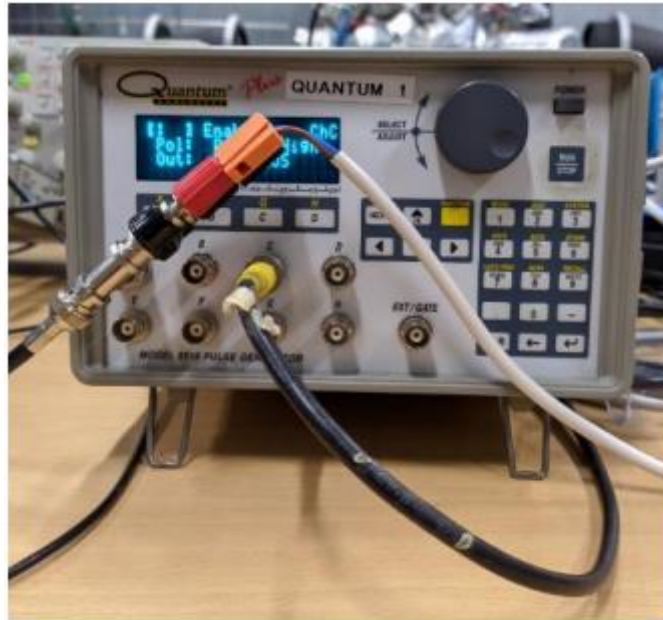
Figure 4.3: Pulse delay generator.

A voltage probe Tektronix P6015A shown in the figure 4.4 is used to measure the voltage at the spark breakdown. The probe enables the oscilloscope and other measuring instruments to have capability of measuring high voltages. Some of the typical electrical characteristics of the probe can be found in here [19].
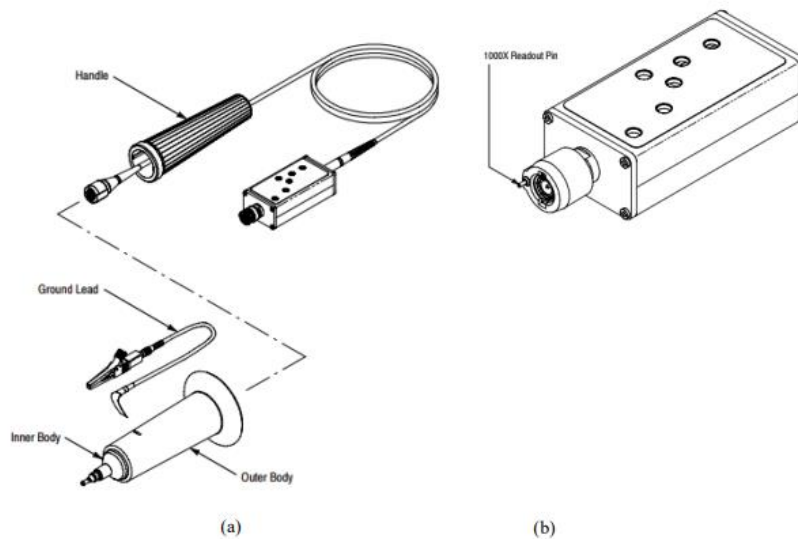
Figure 4.4: Tektronix P6015A high voltage probe [36]: (a) Modules of probe, (b) Compensation box [19]

Power supply to the electrical circuit set up was provided by a laboratory power supply GW Instek GPS-3030 represented in figure 4.5 with single output DC power output equal 90 W, 3A, 30V. More relevant and technical specification can be found in the product document [20]

Figure 4.5: DC Power Supply GW Instek GPS-3030

Mascot Electronics model 719 shown in figure 4.6, an AC/DC linear regulated laboratory power supply which is used to supply voltage to the circuit. The technical rating of the model is 15V, 2A, max 45 W. More technical specification and details are given in product document [21].

SSR-10 DD model or relay shown in figure 4.6 is used to connect the power supply, pulse generator and high-voltage supply. The control method on which the relay works is something called Isolated by Photo couple and the input operating voltage of the relay is 3-32 VDC whereas the output operating voltage is 5-60 VDC. More technical of the relay model can be found in the product description [22].

Figure 4.6: Mascot power supply and solid-state relay

The probe discussed above is connected to equipment called oscilloscope shown in figure 4.7, to digitalize the current and voltage data signal recorded during the breakdown voltage at the electrodes during the execution of the experiments. The display in the oscilloscopes displays data signals which can be analyzed to determine the properties like noise, frequency, time interval amplitude etc. of a signal. The lab setup at the USN has three oscilloscopes where the first oscilloscope is shows the voltage drop signal which determines whether there was spark or not. The second oscilloscope displays the voltage and scaled current signal which is further analyzed to determine the ignition or spark energy. And the third oscilloscope is used to display the pressure signals which can determine whether ignition occurred or not. Since the temperature of the explosion is not noted upon triggering of the spark, it's a situation where it cannot be said whether a ignition has occurred or not. Therefore, rise in the pressure signal in the oscilloscope three it can be determined that an ignition has occurred. The rise in pressure is due to the combustion of the hydrogen mixture filled inside the explosion sphere. More technical of the oscilloscope model can be found in the product document [23].
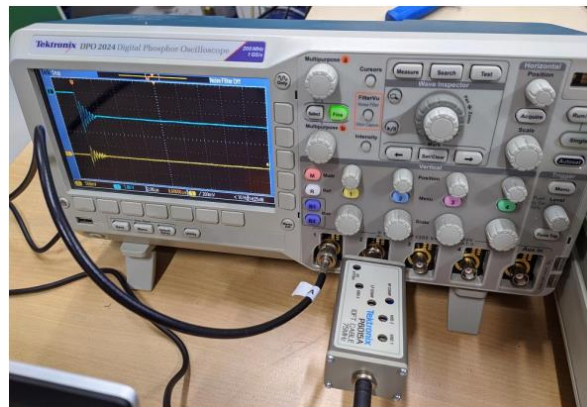
Figure 4.7: Oscilloscope Tektronix DPO 2024

Two type 5011B Kistler single channel multi range laboratory charge amplifier is used in the experimental setup which have their application in measuring the mechanical quantities e.g., Pressure force, acceleration. The amplifiers have large measuring range along with wide frequency range and adjustable low pass filter. Figure 4.7 displays the amplifiers used.

Figure 4.7: Type 5011B amplifier.

The electrical setup also has a current transducer Magnelab CT-C-1.0-BNC shown in the figure 4.8. This current transducer has operating temperature of -20°C to +120°C with higher nominal accuracy ±0.5% over a broad bandwidth. In addition, the output voltage ranges from .025 to 5.0 V/A. The current transducer also packs some other features such as, its 5 times more sensitive to low intensity signal measurement, has higher frequency cutoff and reliable rendering of fast transients. More technical specifications can be found in the product documentation [24]

Figure 4.8: Current transducer.

4.2 Explosion sphere.

A standard 20 Liter explosion sphere is used to determine the spark ignition made by Anko. It's made of double layer stainless steel and can be shown on figure 4.9 and figure 4.10 (a). The explosion sphere is insulated with insulating glass wool and then with aluminum foil to reduce the heat loss and maintain the desired temperature inside the vessel as per the experiment requirements. The explosion sphere is equipped with following mechanisms and characteristics. The maximum working pressure of the sphere of the explosion sphere is 40 bar while the maximum measuring range is 0-25 bar [25].

1. 0.1m windows located on two parallel walls to visually observe ignition
2. Mixing propeller ensures a homogeneous of mixture
3. Kistler pressure transducer measures transient pressure during combustion
4. Keller pressure transducer controls filling process
5. Liquid evaporator evaporates liquid
6. Liquid sample tube supplies liquid fuel from port to evaporator
7. Spark igniter produces sparks to ignite mixture.
8. Ambient temperature probe checks outside temperature
9. Liquid injection port, gas injection port and air injection port supply liquid, gas, and air, respectively
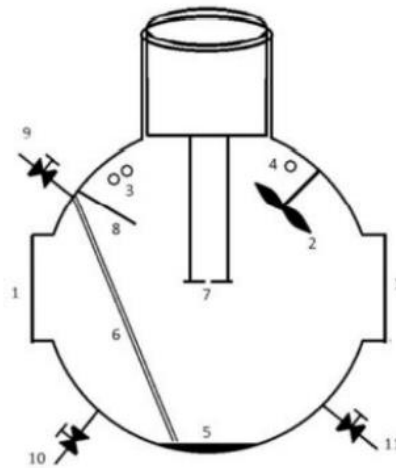
Figure 4.9: Schematic Explosion sphere [25].
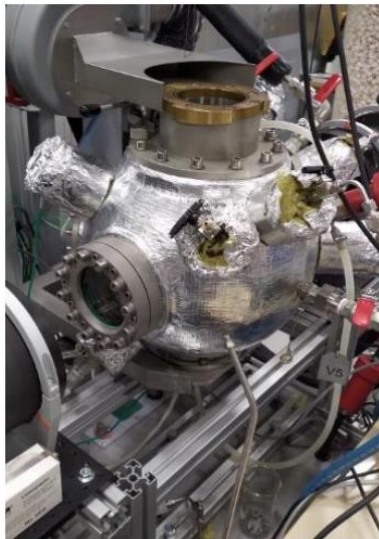
(a)

(b)

Figure 4.10: (a) Explosion sphere, (b) Operating Panel

The explosion sphere has a lid which can be opened to access the electrodes attached to it. The spark ignition circuit discussed above is connected to the explosion sphere's lid and then through it to spark electrodes inside of sphere's lid to ignite mixture. The concentration of flammable mixture filled inside the explosion sphere is determined by the partial pressures of fuel (H_2) and air (N_2, O_2). The operating panel for the explosion sphere is shown in figure 4.10 (b).

4.3 Schlieren Visualization

To determine whether a proper ignition of the mixture took inside the explosion, we can determine it through the pressure readings in the oscilloscope 3. But a better way to observe the phenomenon can be using a visualization system and the ability to record it. And therefore, a Schlieren Visualization setup is used in order to capture the phenomenon of the spark ignition and further visualize it to determine how the ignition took place by looking at the shock waves which can further be used to calculate the burning velocities of the hydrogen mixtures.

"The basic principle of the schlieren technique is the optical projection of an object with an indication of its light deflection" given by the German physicist August Toepler [26].

The phenomenon of Schlieren Visualization is mainly based on the difference in air density. Light refracts when it passes through materials with different densities. The diagram in figure 4.11 shows a typical schlieren visualization system with a point light source.
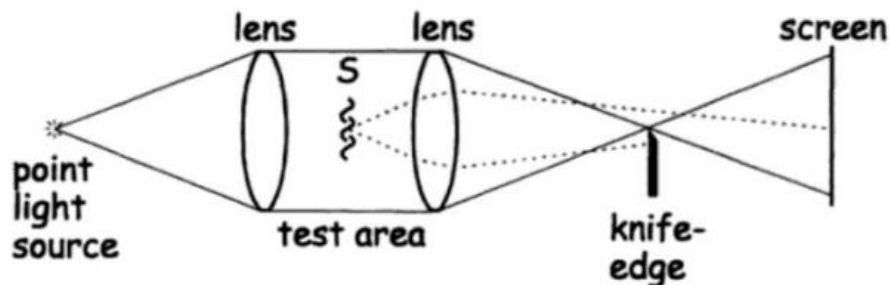
Figure 4.11: Typical schlieren visualization

The setup used in the USN laboratory has a provision where it's possible to have a view inside the explosion sphere through the windows which are 10mm in diameter using light source. Figure 4.12 shows the setup placed in USN laboratory.
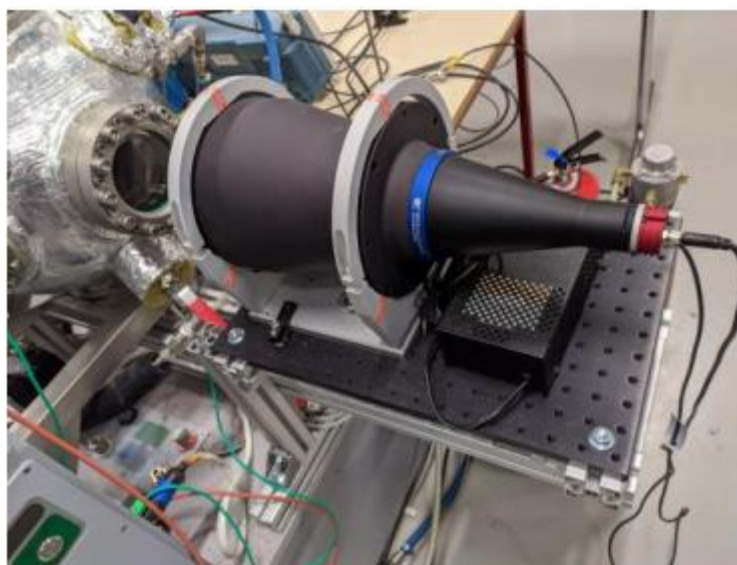
Figure 4.12: Light source

A high speed Kirana video camera is mounted on the other side of the explosion sphere as shown in figure 4.13 which was used to record the schlieren images at the rate of 5K-50K (varying as per different tests conducted) frames per second at a resolution 924 x 768 with feature for pre and post event triggering. The camera was connected to the laboratory laptop on which the recorded films of the spark ignition can be analyzed in terms how well the ignition proceeded. Further, these recorded films can be used to trace and determine the burning velocities of the fuel mixtures using coding scripts.

Figure 4.12: Kirana high speed camera.

5 Experimental Procedure

The experimental procedure attached is in Appendix A. shows the lab sheet used to record the data while performing the experiments on the lab day. It also has safety instructions followed before and after the experiments are done. By following the instructions given at the start, a complete ignition system can be set up such as starting the compressor, fume extractor, etc. also safety measures can be ensured against probable risks. To set up the ignition explosion sphere temperature should be set. The ambient pressure logger is stated through computer software to record the explosion sphere pressure. All the valves except V3 and V4 should be closed. The vacuum pump is started from the control panel which drops the pressure to desirable pressure inside the explosion sphere approximately 100 mbar, which is then noted. Upon achieving the desired pressure vacuum pump should be stopped. An approx. value of 100 mbar is desirable because it's then easy to keep the concentration in check and calculation becomes a little easier. Then as per the requirement of the experiment the fuel (H2), Nitrogen and air are filled inside the explosion sphere. Please refer to the excel sheet in Appendix E for the calculation of hydrogen mixtures determined by changing the phi and lambda. Upon filling the desired mixtures in the explosion sphere the pressure inside it reaches near 1bar and then a stirrer is activated from the control panel to mix the different gases properly for 5 minutes. The end temperature of the explosion sphere is noted which is also the temperature of the mixture. After the stirring, the mixture is allowed to rest for 3 minutes and meanwhile, the other equipment such as electrical circuit (sensor and capacitor), data acquisition systems (Oscilloscopes), high-speed camera settings on the laptop, and pulse generator are prepared to record the ignition. Final pressure on the laptop then can be observed and noted once the ambient pressure logger has been stopped after 3 minutes timer has stopped. It's now important to check that all the values are closed so that ignition can be triggered. Once the ignition is triggered fume extractor is started from the control panel and values of the ambient air and flushing outlet (V5 and V6) are opened. The flushing continues for about 5 mins and once the 5- minute timer stops the fume extractor can be stopped and the valves V5 and V6 can be closed. Meanwhile, all the recorded data from oscilloscopes and the high-speed camera recording along with the pressure logger data is saved. For oscilloscopes: click on the save button so that data is saved to the pen drives. For Kirana high-speed video camera: Save as AVI and RAW format. It is necessary to shut down the whole system after each experiment by following the instructions in Appendix A.

Likewise, all the experiments are to be recorded and data is noted in Appendix A and then saved in Appendix F. Upcoming chapters will focus more on the data taken and results observed after the data analysis. It is important to mention that all the experiments and the data recorded for it were performed under normal conditions.

6 Result and Discussion

This chapter contains the results observed from the experiments done. Data from the Oscilloscopes were analyzed using MATLAB scripts in Appendix B, C, and D. And then further calculation was registered to Appendix G. The results discussed in this chapter correspond to project SJa_P102.

6.1 Oscilloscope Signals

The oscilloscope generates pulse signal data shown in figure 6.1 when the electrical circuit is triggered. Oscilloscope 1 shows the voltage drop and helps in determining the charging of the capacitor and then triggering of spark. Below is a figure from the Oscilloscope 1 for experiment 22_SJa_P102_T00036 where a capacitor of 20nF is charged for 1000 ms and then discharged to have a single spark (since the voltage drop is only seen once).
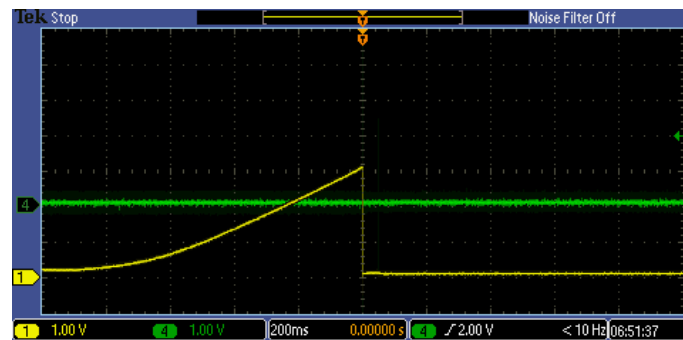
Figure 6.1: Signal generated on Oscilloscope 1.

Oscilloscope 2 generates a slightly different pulse signal data namely the potential and the scaled current plot is shown in figure 6.2 when the Ignition system is triggered. Channel 1 and Channel 3 are used to connect the probes for sensing potential and scaled current signals respectively. Figure 6.2 potential and scaled current data collected by Oscilloscope 2 for experiment 22_SJa_P102_T00036 where the value of λ and φ determining the concentration values of the mixture were 0.5 and 1 respectively.
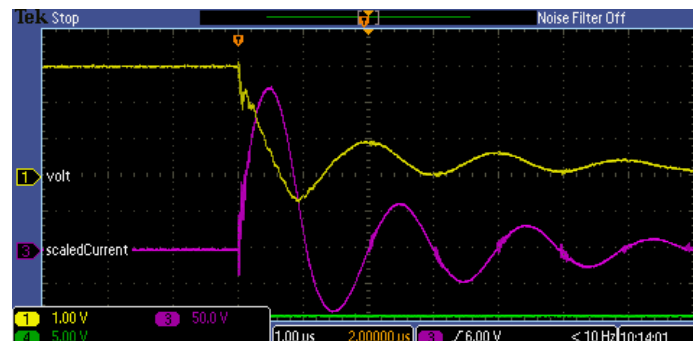
Figure 6.2: Signal generated on Oscilloscope 2.

Oscilloscope 3 provides pressure rise readings inside the Explosion sphere which indicates a successful ignition since the pressure rise inside the explosion sphere is due to the burnt-up mixture of the hydrogen-air mixture.

6.2 Processed plots.

The signal plots available from oscilloscope 2 are then processed using MATLAB scripts where the csv file generated from the is first converted to a .mat file (Appendix B) which is much easier for MATLAB to read and take data from for further analysis. Another MATLAB code (Appendix C) was then developed and used to process the .mat file to plot the data collected by the Oscilloscopes.

6.2.1 Current vs Time

Figure 6.3 shows the plot of the scaled current data from oscilloscope 2 when processed through the MATLAB code (Appendix C). A new range is defined to limit the range of data for further calculation of spark energy. Initially, the new range I3 has an offset and noise which is then corrected as adjusted I3 and then filtered adjusted I3 when passed through a lowpass filter. Here a typical sine wave is observed for scaled current when the ignition is triggered when the capacitor is charged up to the desired voltage. Through indexing peak values of current can be obtained which was 223.58 A.
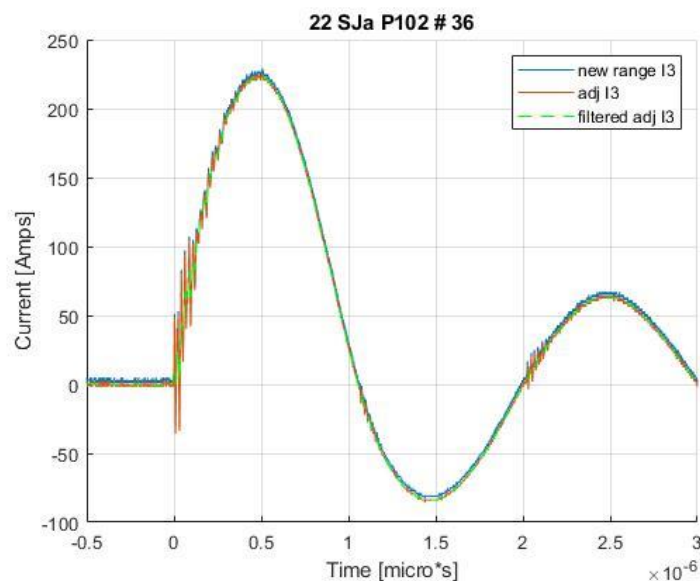
Figure 6.3: Current vs Time

6.2.2 Potential vs Time

Figure 6.4 shows the new range potential plot obtained as same as the scaled current plot. The time scale for both scaled current I3 and potential is kept the same to plot the spark energy data in the same time scale range. The degree of the filter can be adjusted by adjusting the lowpass filter value. The dramatic slope curve in the potential plot shows the phenomenon of spark

triggering upon discharging of the capacitor of 20 nF used in this test. Through Indexing, Peak voltage for the test 22_SJa_P102_T00036 was determined to be 3.22 kV.
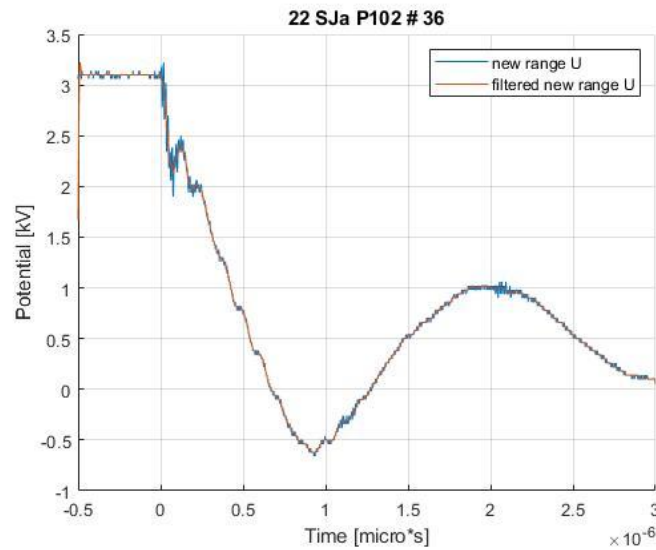
Figure 6.4: Potential vs Time

6.2.3 Combined Plot

Figure (6.5) shows the Potential, Current, and different Spark energies on the same plot vs the time scale. The spark energy cumulative is obtained through numerical integration of the discrete data range set. Similarly, spark energy is also calculated using the trapezium method of integration which gives a single value of spark energy that is the same as the last value of the cumulative energy. Other spark energies for the test are plotted on different instances by obtaining Indices when Current is maximum, Zero for the second time. This plot helps in analyzing the variations simultaneously. In Appendix G, spark energy at Uzero is missing for the following tests P102_T00001 to P102_T00006 and P102_T00011 to P102_T00016 because the potential plot doesn't pass through the zero indexes on the x-axis.
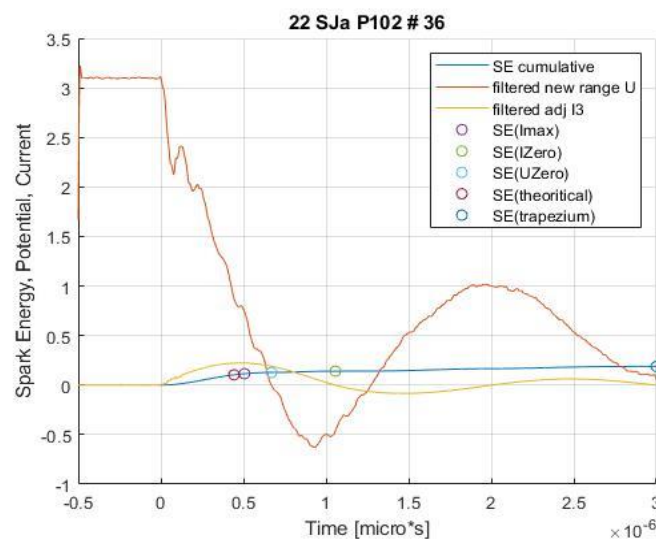
Figure 6.5: Spark energy, Potential, current vs Time

6.2.4 Spark Energies vs Time

Figure 6.6 shows all the spark energies plotted at different instances through the spark triggering. The curve shows how the spark energy increases with time for the given range of data until the signal dies out. It might be confusing to see that spark energy at Imax is less than Izero 0.11 and 0.14 mJ respectively, since the spark energy Izero is calculated when the current plot hits zero after it has achieved a peak value a fraction of time has passed with adds to the spark energy at IZero index. The difference between the theoretical and the calculated value through numerical integration can be found more clearly on this plot.

The values of spark energies at Imax, Izero, Uzero, Theoretical and cumulative for the test 22_SJa_P102_T00036 were found out to be 0.11, 0.14, 0.10, 0.12, 0.18 mJ respectively

Theoretical Spark energy is calculated using the capacitance spark energy formula equation 2.2, while experimental/cumulative spark energy is calculated using numerical integration. This difference in both the values can mean that the system has a fraction of capacitance which induces additional capacitance energy than that is provided. Also, it was observed that this difference is surprisingly less when the ignition circuit uses a high capacitor.
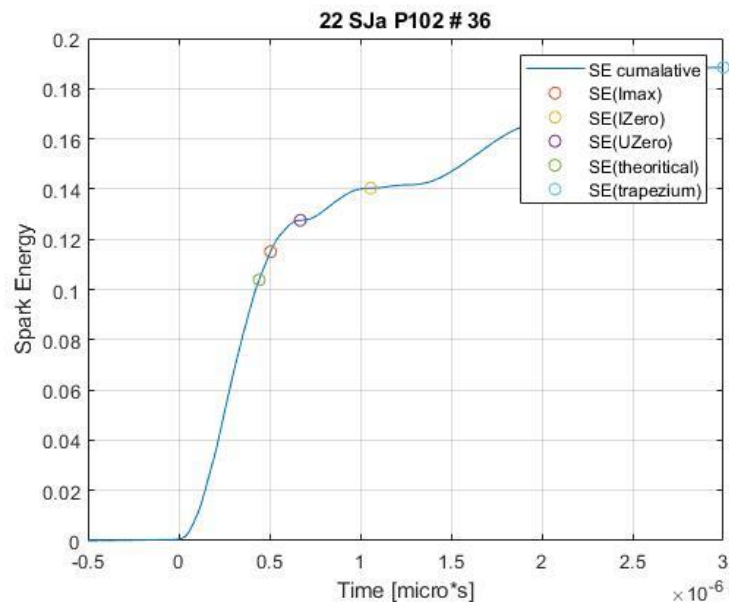
Figure 6.5: Spark Energies vs Time

6.2.5 Spark energy results

Table 6.1 and Table 6.2 represents the spark energy data for theoretical and experimental calculation when phi is 1.0 and 0.8 respectively. In the table only the test in which a proper ignition was observed is mentioned with the least available capacitor at the USN laboratory.

Table 6.1: Phi equal to 1

Sno.	Test No.	Target Lambda (λ)	Actual Lambda (λ)	Capacitor rating [pF]	Spark energy Cumulative /experimental [mJ]	Spark energy Theoretical [mJ]
1	12	1	1	10	0.02155	0.00007
2	13	0.8	0.8	10	0.02228	0.00007
3	14	0.6	0.6	10	0.02547	0.00009
4	40	0.5	0.5	5000	0.06526	0.02475

Table 6.2: Phi equal to 0.8

Sno.	Test No.	Target Lambda (λ)	Actual Lambda (λ)	Capacitor rating [pF]	Spark energy Cumulative /experimental [mJ]	Spark energy Theoretical [mJ]
1	47	1	1	100	0.01659	0.00054
2	48	0.8	0.8	100	0.02550	0.00085
3	70	0.6	0.6	100	0.01690	0.00056
4	71	0.5	0.5	100	0.02015	0.00069
5	69	0.4	0.39	30,000	0.27012	0.16047

6.2.6 Fuel – Air and Fuel – Oxygen Equilibrium

Equation 6.1 is the simplified governing reaction for the hydrogen-air mixture.

$$\Phi H_2 + \frac{\lambda}{2} O_2 + \frac{1}{2} (4.76 - \lambda) N_2 \tag{6.1}$$
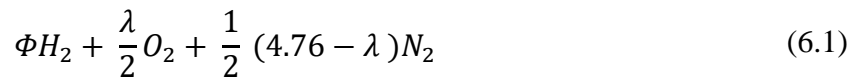
Fuel – Air Equilibrium is represented by equation 6.2. Whereas Fuel – Oxygen Equilibrium is represented by equation 6.3.

$$\Phi_{Air} = \frac{\dfrac{F}{A}}{\dfrac{F}{A_{St}}} \tag{6.2}$$

$$\Phi_{O_2} = \frac{\dfrac{F}{O}}{\dfrac{F}{O_{St}}} \tag{6.3}$$

While air-fuel ratio λ can be represented as equation 6.4

$$\lambda = \frac{\Phi_{Air}}{\Phi_{O_2}}$$

(6.4)

Table 6.3: Actual vs Targeted λ and corresponding Φ_{Air} and Φ_{O_2}

Sno.	Test No.	Target Phi Φ	Target Lambda (λ)	Actual Lambda (λ)	Corresponding Fuel – Air Equilibrium Φ_{Air}	Corresponding Fuel – O2 Equilibrium Φ_{O_2}
1	47	0.8	1	1	0.8	0.8
2	48	0.8	0.8	0.8	0.82	1.03
3	70	0.8	0.6	0.6	0.81	1.36
4	71	0.8	0.5	0.5	0.81	1.63
5	69	0.8	0.4	0.39	0.80	2.04
6	12	1	1	1	0.99	0.99
7	13	1	0.8	0.8	0.99	1.24
8	14	1	0.6	0.6	0.99	1.65
9	40	1	0.5	0.5	1.00	2.01

The idea behind the equations 6.1, 6.2, 6.3, and 6.4 is to provide a way to check whether the calculated or actual air-fuel ratio λ is correct or not. Table 6.3 represents such data which is calculated using this set of equations in the result sheet Appendix G.

7 Conclusions

Figure 7.1 shows the status of the tests and whether they were properly ignited, partially ignited or didn't ignite at all. The blue color mark shows the tests where the hydrogen mixture successfully ignited. It can be interpreted that the test which had a balanced air-fuel ratio ignited by less energy input whereas tests which had concentrations where the air-fuel ratio was thin mainly with less oxygen required high spark energy.
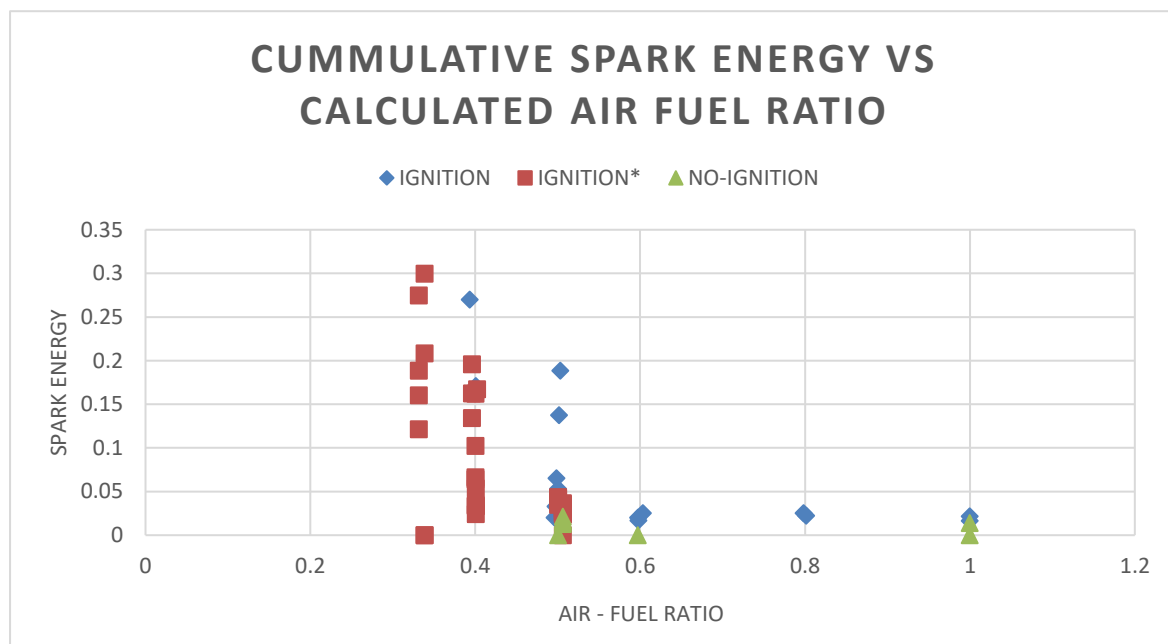
Figure 7.1: Spark energy vs λ

In table 6.2 it can be observed that the spark energy varies a little even when the capacitance used and charge time are the same. This can be due to the residual charge in the capacitor or the capacitance of the high voltage supply XP EMCO model Q101-5.

A slight variation can also be observed in a few experiments for the value of lambda and Phi in the Appendix G. This can be due to slight variations in partial pressure while filling the gases into the explosion sphere. But From test 58 to 65 the target value and actual calculated value of lambda start to deviate because of an error in nitrogen partial pressure while filling which was supposed to 449 but read as 499 mbar.

Often it might seem that capacitor is used as the basis to factor in the spark energy for the given concentration but no linear relation cannot be established when the value of air-fuel ratio λ keeps changing.

The results in appendix G show the spark energy at different concentrations of the hydrogen mixture but the sensitivity of the experimental setup doubts whether the calculated spark energy can be considered as the minimum energy or not.

As far as the objective of this thesis is concerned, various research work done over the year was gone through in the second chapter, and factors influencing the spark energy were covered in the third chapter. Successfully experiments were conducted which produced reliable results were produced but one objective of modeling the ignition circuit in Simulink was only partially done.
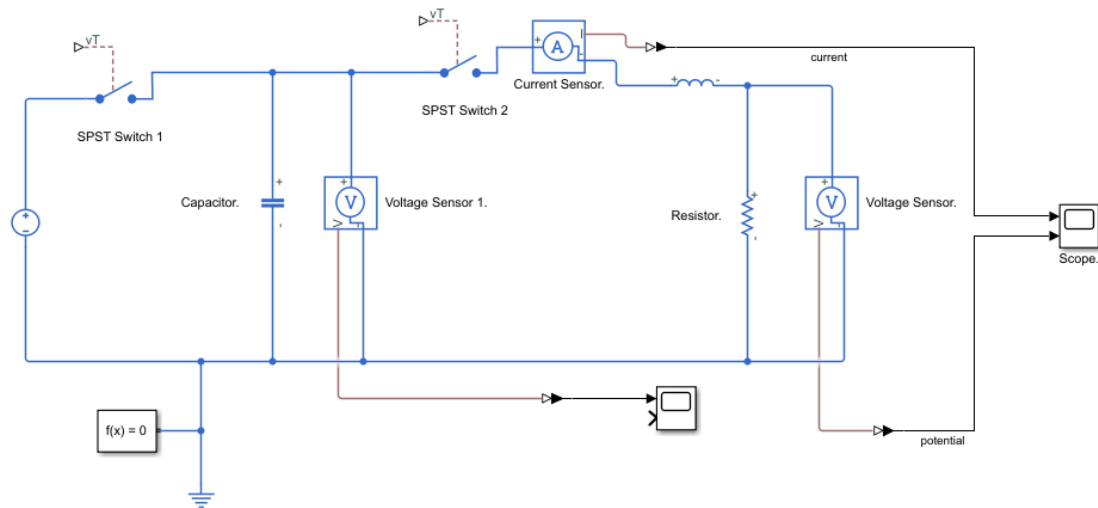
Figure 7.2: Simulink model of the ignition circuit

References

[1]   "Green Steel Production – How G7 Countries Can Help Change the Global Landscape." https://www.industrytransition.org/insights/g7-green-steel-production/ (accessed May 17, 2022).

[2]   International Energy Agency, *Global Hydrogen Review 2021*. OECD, 2021. doi: 10.1787/39351842-en.

[3]   "Addressing hydrogen safety challenges: what should we be aware of?," *Gexcon AS - Fire & Explosion Consultants*. https://www.gexcon.com/blog/addressing-hydrogen-safety-challenges/ (accessed May 17, 2022).

[4]   G. Vislie, "Key Learning points from Hydrogen Incident.," *Gexcon*, p. 15.

[5]   "CEM Hydrogen Initiative – Programmes," *IEA*. https://www.iea.org/programmes/cem-hydrogen-initiative (accessed May 17, 2022).

[6]   S. McAllister, J.-Y. Chen, and A. C. Fernandez-Pello, *Fundamentals of Combustion Processes*. New York, NY: Springer New York, 2011. doi: 10.1007/978-1-4419-7943-8.

[7]   B. Lewis and G. Von Elbe, *Combustion, flames, and explosions of gases*, 3rd ed. Orlando: Academic Press, 1987.

[8]   R. K. Eckhoff, M. Ngo, and W. Olsen, "On the minimum ignition energy (MIE) for propane/air," *J. Hazard. Mater.*, vol. 175, no. 1, pp. 293–297, Mar. 2010, doi: 10.1016/j.jhazmat.2009.09.162.

[9]   E. Randeberg and R. K. Eckhoff, "Measurement of minimum ignition energies of dust clouds in the <1mJ region," *J. Hazard. Mater.*, vol. 140, no. 1–2, pp. 237–244, Feb. 2007, doi: 10.1016/j.jhazmat.2006.06.102.

[10]   M. Kono, K. Iinuma, S. I. Kumagai, and T. Sakai, "Spark Discharge Characteristics and Igniting Ability of Capacitor Discharge Ignition Systems," *Combust. Sci. Technol.*, vol. 19, no. 1–2, pp. 13–18, Nov. 1978, doi: 10.1080/00102207808946859.

[11]   R. Ono, M. Nifuku, S. Fujiwara, S. Horiguchi, and T. Oda, "Minimum ignition energy of hydrogen–air mixture: Effects of humidity and spark duration," *J. Electrost.*, vol. 65, no. 2, pp. 87–93, Feb. 2007, doi: 10.1016/j.elstat.2006.07.004.

[12]   G. Cui, W. Zeng, Z. Li, Y. Fu, H. Li, and J. Chen, "Experimental study of minimum ignition energy of methane/air mixtures at elevated temperatures and pressures," *Fuel*, vol. 175, pp. 257–263, Jul. 2016, doi: 10.1016/j.fuel.2016.02.025.

[13]   G. Lüttgens and N. Wilson, *Electrostatic hazards*. Oxford ; Boston: Butterworth Heinemann, 1997.

[14]   "Paschen's law," *Wikipedia*. Mar. 31, 2022. Accessed: May 18, 2022. [Online]. Available: https://en.wikipedia.org/w/index.php?title=Paschen%27s_law&oldid=1080258746

[15]   J. Liu, M. Bi, H. Jiang, and W. Gao, "Evaluation of spark discharge," *J. Electrost.*, vol. 107, p. 103500, Sep. 2020, doi: 10.1016/j.elstat.2020.103500.

[16]   R. K. Eckhoff, *Explosion hazards in the process industries*, 2nd edition. Waltham, MA: Elsevier, 2016.

[17]   S. P. M. Bane, J. L. Ziegler, and J. E. Shepherd, "Investigation of the effect of electrode geometry on spark ignition," *Combust. Flame*, vol. 162, no. 2, pp. 462–469, Feb. 2015, doi: 10.1016/j.combustflame.2014.07.017.

[18]   A. Wähner, G. Gramse, T. Langer, and M. Beyer, "Determination of the minimum ignition energy on the basis of a statistical approach," *J. Loss Prev. Process Ind.*, vol. 26, no. 6, pp. 1655–1660, Nov. 2013, doi: 10.1016/j.jlp.2013.06.002.

[19]   "P6015A | Tektronix." https://www.tek.com/en/high-voltage-probe-manual/p6015a (accessed May 18, 2022).

[20]   D. by A. S. | www.akacia.com.tw, "GPS-Series Linear D.C. Power Supply." https://www.gwinstek.com/en-global/products/detail/GPS-Series (accessed May 18, 2022).

[21]   "MASCOT 719 | Mascot Bench Top Power Supply, 15V, 2A, 45W, Adjustable," *Distrelec Norway*. https://www.elfadistrelec.no/en/bench-top-power-supply-15v-2a-45w-adjustable-mascot-mascot-719/p/16984306 (accessed May 18, 2022).

[22]   "FOTEK- SSR-10DD Solid State Relay." http://www.photosensor.com.tw/Solid%20State%20Relay/Single%20Phase%20Solid%20State%20Relay%20(DC%20to%20DC%20SSR)/SSR-10DD.htm (accessed May 18, 2022).

[23]   "DPO2024 Tektronix | Mouser," *Mouser Electronics*. https://no.mouser.com/ProductDetail/795-DPO2024 (accessed May 18, 2022).

[24]   "HFCT Current Transformer Broad Frequency Response Magnelab," *Magnelab*. https://www.magnelab.com/products/ac-current-transformer-broad-frequency-response-hfct/ (accessed May 18, 2022).

[25]   M. Henriksen, K. Vaagsaether, J. Lundberg, S. Forseth, and D. Bjerketvedt, "Explosion characteristics for Li-ion battery electrolytes at elevated temperatures," *J. Hazard. Mater.*, vol. 371, pp. 1–7, Jun. 2019, doi: 10.1016/j.jhazmat.2019.02.108.

[26]   "Schlieren," *Wikipedia*. Mar. 09, 2022. Accessed: May 18, 2022. [Online]. Available: https://en.wikipedia.org/w/index.php?title=Schlieren&oldid=1076027194

Appendices

Appendix A – Laboratory log sheet

Appendix B – MATLAB script for .mat file conversion

Appendix C – MATLAB script for Oscilloscope data analysis and Plotting.

Appendix D – MATLAB script for reading the input sheet and writing in result sheet excel.

Appendix E – Partial Pressure calculation sheet.

Appendix F – Data Input Sheet

Appendix G – Data Result Sheet

Appendix A – Laboratory log sheet

Safety checklist and results matrix for explosion sphere experiments.

Date: 3. 02 22   Project Number: P/02

01 – Protection gear	✓	✓ 06 – Check Air compressor or outlet	✓
02 – Check fire extinguisher	✓	✓ 07 – Start all sensors and the explosion sphere	✓
03 – Start ventilation		✓ 07 – Start data acquisition systems	✓
04 – Check state of explosion sphere		✓ 09 – Tighten explosion sphere lid.	✓
05 – Prepare gas cylinder /chemical		✓ 10 – Start camera and light (lens cover)	✓

Note: **All valves** are all valves except **v1 and v2** (the valves for heating cap).

Name of experiment	T01	T02	T03	T04	T05
Time	12:40 PM	1:10 PM	1:40PM		↑
Type of fuel	Hydrogen	H2	H2		
Concentration target	10 /.	10 /.	8 /.		
Set vessel temperature	27°C / 200K	27°C	26.9		
Start ambient pressure logger	✓	✓	✓	Same as T04	Same as T04
Close all valves	✓	✓	✓		
Open V3 and V4	✓	✓	✓		
Start vacuum pump	✓	✓	✓		
Close V3 at desired pressure	✓	✓	✓		
Stop vacuum pump	✓	✓	✓		
Initial Pressure	99.9	100.4	100.6		
Add Fuel	✓	✓	✓	as T03	
Partial Pressure with Fuel	373.9	203.9	180.1		
Start stirrer	✓	✓	✓		
Add oxidizer	✓	✓	✓		
Start timer (5 min)	✓	✓	✓		
Stop stirrer	✓	✓	✓	T03	
End Temperature	26.9	27.0	27.1		
Start timer (3 min)	✓	✓	✓		
Capacitor [pF]	10 PF	10 PF	10 pF		100 pF
Voltage Power Supply [V]	5 V	5 V	5 V		5 V
Charge Time HV [ms]	40 ms	40 ms (50ms)	50 ms		80 ms
Total Pressure	1001.0	999.5	1001.0		
Close V4	✓	✓	✓		
Stop ambient pressure logger	✓	✓	✓		
Check that all valves are closed	✓	✓	✓		
Connect igniter	✓	✓	✓	✓	
Ignite mixture	✓	✓	✓		✓
Ignition (Yes/No)	Yes	yes	NO.	NO	No Yes
Disconnect igniter	–	–	–	–	–
Start Fume extractor	✓	✓			✓
Open V6 and V5	✓	✓			✓
Flush system (5 min)	✓	✓			✓
Close V6 and V5	✓	✓			✓
Stop fume extractor	✓	✓			✓
Save all data	✓	✓		✓	✓

01 – Shut down compressor and gas supply	✓	05 – Turn off lamp power unit	✓
02 – Shut down computers	✓	06 – Cover lenses and mirrors	✓
03 – Turn off explosion sphere	✓	07 – Open explosion sphere lid	✓
04 – Turn off camera	✓	08 – Stop ventilation	✓

Remember to write any comments or remarks in the logbook

Appendix B – MATLAB script for .mat file conversion

```matlab
%
close all; clear;

test = (30);

for i = 1:length (test)

    test (i);
    Num = num2str(test(i));
    pathname = '22_SJa_P102_T00000';
    pathname(19-length(Num):18) = Num;
    filename = '22_SJa_P102_TS0000.csv';
    filename(19-length(Num):18) = Num;

    table = readtable([pathname '/'
filename],'HeaderLines',15);  % Read from line 15

    t = table {:,1};
    U = 1000.*table{:,2}; % 1000 x probe / scale*volt /
str2double(T{9,2}).*
    I3 = table{:,3};     % scale*volt / 1 V/A current sensor @
1 M ohm and 10 x probe ?????
    I4 = table{:,4};

    newfilename = filename(1:18);
    newfilename(14) = 'D';

    save([pathname,'/',
newfilename,'.mat'],'t','U','I3','I4');

end
```

Appendix C – MATLAB script for Oscilloscope data analysis and Plotting

```matlab
%
close all;
clear ;

test = (36);

for i = 1  : length(test)

    Num = num2str(test(i));
    pathname = '22_SJa_P102_T00000';
    pathname(19-length(Num):18)  = Num;
    filename = '22_SJa_P102_TD0000';
    filename(19-length(Num):18)  = Num;

    load([pathname,'/', filename,'.mat'],'t','U','I3','I4');

end

startpoint_1 = find(t==-0.5*1e-6);
endpoint_1 = find(t==3*1e-6);
new_Range_t = t(startpoint_1:endpoint_1);
new_range_I3 = I3(startpoint_1:endpoint_1);
adj_I3 = new_range_I3 - mean(I3(1:startpoint_1));
filtered_adj_I3=lowpass(adj_I3,1,1000);

% plotting scaled current and time
figure (1)
grid on
hold on
plot (new_Range_t,new_range_I3)
plot (new_Range_t,adj_I3)
plot (new_Range_t,filtered_adj_I3,'--g')
legend ('new range I3','adj I3','filtered adj I3')
hold off
title(['22 SJa P102 # ',num2str(test)])
xlabel('Time [micro*s]')
ylabel('Current [Amps]')

% ploting Potential and Time
new_range_U = U(startpoint_1:endpoint_1);
filtered_new_range_U=lowpass(new_range_U,1,1000);

figure (2)
hold on
plot (new_Range_t,new_range_U.*1e-3)
```

```matlab
grid on
plot (new_Range_t,filtered_new_range_U.*1e-3)
legend ('new range U','filtered new range U')
title(['22 SJa P102 # ',num2str(test)])
xlabel('Time [micro*s]')
ylabel('Potential [kV]')


% [minU] = min(filtered_new_range_U) ;  % min U
[maxU] = max(filtered_new_range_U) ;  % max U
[minU] = 0;

% [absminU] = abs(min(filtered_new_range_U)) ;  % abs min U
% [absmaxU] = abs(max(filtered_new_range_U)) ;  % abs max U

absolute_current = abs (filtered_adj_I3);  % absolute value of
current
absolute_potential = abs (filtered_new_range_U);  % absolute
value of potential

absPower = absolute_potential.*absolute_current; % power with
absolute values

MIE = cumtrapz (new_Range_t,absPower);  %cumtrapz method
MIE_1 = trapz (new_Range_t, absPower);  % trapz method

ImaxIdx=find(filtered_adj_I3 ==
max(filtered_adj_I3),1,'first');
Imax=filtered_adj_I3(ImaxIdx);
MIE_Imax = MIE(ImaxIdx);
IZeroIdx=ImaxIdx+find(filtered_adj_I3(ImaxIdx:end) <=
0,1,'first');
MIE_IZero = MIE(IZeroIdx);

UZeroIdx=find(filtered_new_range_U <= 0,1,'first');
MIE_UZero = MIE(UZeroIdx);

C = 20000; % capacitance used in experiment
MIE_2 = 0.5*C*10^-12*((maxU - minU)^2); % Energy using energy
expression % E=0.5*C*V^2

tol = 0.0001;
MIEIdx = find(abs(MIE_2 - MIE) <= tol);
MIE_th = MIE(MIEIdx);

MIE_1Idx = find(MIE == max(MIE),1,'first');
MIE_1trapz = MIE(MIE_1Idx);
%
figure (3)
```

```matlab
grid on
hold on
plot (new_Range_t,MIE)
plot (new_Range_t,filtered_new_range_U.*1e-3)
plot (new_Range_t,filtered_adj_I3.*1e-3)
plot
(new_Range_t(ImaxIdx),MIE(ImaxIdx),'o',new_Range_t(IZeroIdx),M
IE(IZeroIdx),'o',new_Range_t(UZeroIdx),MIE(UZeroIdx),'o')
plot
(new_Range_t(MIEIdx),MIE_th,'o',new_Range_t(MIE_1Idx),MIE_1tra
pz,'o')
hold off
legend ('SE cumulative','filtered new range U','filtered adj
I3','SE(Imax)','SE(IZero)','SE(UZero)','SE(theoritical)','SE(t
rapezium)')
title(['22 SJa P102 # ',num2str(test)])
xlabel('Time [micro*s]')
ylabel('Spark Energy, Potential, Current')
%
figure (4)
plot
(new_Range_t,MIE,new_Range_t(ImaxIdx),MIE(ImaxIdx),'o',new_Ran
ge_t(IZeroIdx),MIE(IZeroIdx),'o',new_Range_t(UZeroIdx),MIE(UZe
roIdx),'o',new_Range_t(MIEIdx),MIE_th,'o',new_Range_t(MIE_1Idx
),MIE_1trapz,'o')
legend ('SE
cumalative','SE(Imax)','SE(IZero)','SE(UZero)','SE(theoritical
)','SE(trapezium)')
title(['22 SJa P102 # ',num2str(test)])
xlabel('Time [micro*s]')
ylabel('Spark Energy')
grid on
```

Appendix D – MATLAB script for reading the input sheet and writing in result sheet excel

```matlab
warning off
resultSheet = readtable('Lab data final.xlsx','Sheet','result
sheet');
inputSheet = readtable('Lab data final.xlsx','Sheet','input
sheet');
endd=length(resultSheet{:,1});
%
noData={'22_SJa_P102_T00001','22_SJa_P102_T00002','22_SJa_P102
_T00003','22_SJa_P102_T00004','22_SJa_P102_T00005','22_SJa_P10
2_T00006','22_SJa_P102_T00011','22_SJa_P102_T00012','22_SJa_P1
02_T00013','22_SJa_P102_T00014','22_SJa_P102_T00015','22_SJa_P
102_T00016','22_SJa_P102_T00031','22_SJa_P102_T00038','22_SJa_
P102_T00046','22_SJa_P102_T00049','22_SJa_P102_T00062','22_SJa
_P102_T00063','22_SJa_P102_T00070','22_SJa_P102_T00071'};
noData={'22_SJa_P102_T00031','22_SJa_P102_T00038','22_SJa_P102
_T00046','22_SJa_P102_T00049','22_SJa_P102_T00062','22_SJa_P10
2_T00063'};

for n = 5:endd % refers to excel sheet row number.
    %"get filename and path"
    projectName = char(table2cell(resultSheet(n,1)));
    testNumber =
num2str(table2array(resultSheet(n,2)),'%0.5i');
    testNumber2 =
num2str(table2array(resultSheet(n,2)),'%0.4i');
    filename = [projectName '_T' testNumber];
    filename2 = [projectName '_TD' testNumber2];
    if any(strcmp(noData,filename))
        continue
    end
    rootPath = 'D:/USN/4th sem/';
    filePath = [rootPath '/' projectName '/' filename];
    %Load mat file in folder
    load([filePath '/' filename2,'.mat'],'t','U','I3','I4');

    %Analyse data
    startpoint_1 = find(t==-0.5*1e-6);
    endpoint_1 = find(t==3*1e-6);
    new_Range_t = t(startpoint_1:endpoint_1);
    new_range_I3 = I3(startpoint_1:endpoint_1);
    adj_I3 = new_range_I3 - mean(I3(1:startpoint_1));
    filtered_adj_I3=lowpass(adj_I3,1,1000);

    % ploting Potential and Time
    new_range_U = U(startpoint_1:endpoint_1);
    filtered_new_range_U=lowpass(new_range_U,1,1000);
```

```matlab
    % [minU] = min(filtered_new_range_U) ;  % min U
    [maxU] = max(filtered_new_range_U) ;  % max U
    [minU] = 0;


    % [absminU] = abs(min(filtered_new_range_U)) ;  % abs min
U
    % [absmaxU] = abs(max(filtered_new_range_U)) ;  % abs max
U

    absolute_current = abs (filtered_adj_I3);  % absolute
value of current
    absolute_potential = abs (filtered_new_range_U);  %
absolute value of potential

    absPower = absolute_potential.*absolute_current; % power
with absolute values

    MIE = cumtrapz (new_Range_t,absPower);  %cumtrapz method
    MIE_1 = trapz (new_Range_t, absPower);  % trapz method

    ImaxIdx=find(filtered_adj_I3 ==
max(filtered_adj_I3),1,'first');
    Imax=filtered_adj_I3(ImaxIdx);
    MIE_Imax = MIE(ImaxIdx);
    IZeroIdx=ImaxIdx+find(filtered_adj_I3(ImaxIdx:end) <=
0,1,'first');
    MIE_IZero = MIE(IZeroIdx);

    UZeroIdx=find(filtered_new_range_U <= 0,1,'first');
    MIE_UZero = MIE(UZeroIdx);

    %C = 20; % capacitance used in experiment
    C = inputSheet{n,13}; % capacitance used in experiment
    MIE_2 = 0.5*C*10^-12*((maxU - minU)^2); % Energy using
energy expression % E=0.5*C*V^2

    tol = 0.0001;
    MIEIdx = find(abs(MIE_2 - MIE) <= tol);
    MIE_th = MIE(MIEIdx);

    MIE_1Idx = find(MIE == max(MIE),1,'first');
    MIE_1trapz = MIE(MIE_1Idx);
    % Write values into table
    resultSheet{n,11}=maxU;
    resultSheet{n,12}=Imax;
    resultSheet{n,13}=C;
    resultSheet{n,14}=MIE_2;
```

```matlab
    resultSheet{n,15}=MIE_1;
    resultSheet{n,16}=MIE_Imax;
    resultSheet{n,17}=MIE_IZero;
%        resultSheet{n,18}=MIE_UZero;
end
% Save new table as excel spreadsheet
writetable(resultSheet, 'finalResults.xlsx')
% writetable(resultSheet,'MIEUZERO.xlsx')
```

Appendix E – Partial Pressure calculation sheet.

Phi	0.5											
lambda	x	y	z	H2	O2	N2	N2/O2	O2/N2		H2[mbar]	Air[mbar]	N2[mbar]
1	1	1	3.76	17.36	17.36	65.28	3.76	0.27		174	826	0
0.8	1	0.8	3.96	17.36	13.89	68.75	4.95	0.20		174	661	165
0.6	1	0.6	4.16	17.36	10.42	72.22	6.93	0.14		174	496	331
0.5	1	0.5	4.26	17.36	8.68	73.96	8.52	0.12		174	413	413
0.4	1	0.4	4.36	17.36	6.94	75.69	10.90	0.09		174	331	496
0.3	1	0.3	4.46	17.36	5.21	77.43	14.87	0.07		174	248	578

.

Appendix F – Data Input Sheet

Project	Test Number	Type of fuel	Concentration target	Target lambda	Total Pressure	Capacitor pF
22_SJa_P101	1	H2	30.00%		1003.1	30
22_SJa_P101	2	H2	12.50%		1003	30
22_SJa_P101	3	H2	12.50%		1003.9	30
22_SJa_P101	4	H2	10.00%		1005.5	30
22_SJa_P102	1	H2	10.00%		1001	10
22_SJa_P102	2	H2	10.00%		999.5	10
22_SJa_P102	3	H2	8.00%		1001	10
22_SJa_P102	4	H2	8.00%		1001	10
22_SJa_P102	5	H2	8.00%		1001	100
22_SJa_P102	6	H2/O2/N2	10%,6%,84%		998.6	100
22_SJa_P102	7	H2/O2/N2	10%,6%,84%		998.7	330
22_SJa_P102	8	H2/O2/N2	10%,6%,84%		998.7	660
22_SJa_P102	9	H2/O2/N2	10%,6%,84%		998.7	1320
22_SJa_P102	10	H2/O2/N2	10%,6%,84%		998.7	2000
22_SJa_P102	11	H2/O2/N2	29.58%,14.79%,55.63%	1	998.3	10
22_SJa_P102	12	H2/O2/N2	29.58%,14.79%,55.63%	1	1002	10
22_SJa_P102	13	H2/O2/N2	29.58%,11.83%,58.59%	0.8	999.4	10
22_SJa_P102	14	H2/O2/N2	29.58%,8.87%,61.55%	0.6	1001.5	10
22_SJa_P102	15	H2/O2/N2	29.58%,7.39%,63.03%	0.5	1001.6	10
22_SJa_P102	16	H2/O2/N2	29.58%,7.39%,63.03%	0.5	1001.6	10
22_SJa_P102	17	H2/O2/N2	29.58%,7.39%,63.03%	0.5	1001.6	330
22_SJa_P102	18	H2/O2/N2	29.58%,7.39%,63.03%	0.5	1001.6	330
22_SJa_P102	19	H2/O2/N2	29.58%,7.39%,63.03%	0.5	1001.6	430
22_SJa_P102	20	H2/O2/N2	29.58%,7.39%,63.03%	0.5	1001.6	430
22_SJa_P102	21	H2/O2/N2	29.58%,7.39%,63.03%	0.5	1001.6	630
22_SJa_P102	22	H2/O2/N2	29.58%,7.39%,63.03%	0.5	1001.6	960
22_SJa_P102	23	H2/O2/N2	29.58%,7.39%,63.03%	0.5	1001.6	1320
22_SJa_P102	24	H2/O2/N2	29.58%,7.39%,63.03%	0.5	1001.6	1650
22_SJa_P102	25	H2/O2/N2	29.58%,7.39%,63.03%	0.5	1001.6	1980
22_SJa_P102	26	H2/O2/N2	29.58%,7.39%,63.03%	0.5	1001.6	2080
22_SJa_P102	27	H2/O2/N2	29.58%,7.39%,63.03%	0.5	1001.6	2080
22_SJa_P102	28	H2/O2/N2	29.58%,7.39%,63.03%	0.5	1001.6	2080
22_SJa_P102	29	H2/O2/N2	29.58%,7.39%,63.03%	0.5	1001.6	2080
22_SJa_P102	30	H2/O2/N2	29.58%,7.39%,63.03%	0.5	1001.6	2080
22_SJa_P102	31	H2/O2/N2	29.58%,7.39%,63.03%	0.5	1001.6	2080
22_SJa_P102	32	H2/O2/N2	29.58%,7.39%,63.03%	0.5	1001.1	2080
22_SJa_P102	33	H2/O2/N2	29.58%,7.39%,63.03%	0.5	1001.1	2080
22_SJa_P102	34	H2/O2/N2	29.58%,7.39%,63.03%	0.5	1001.1	2080
22_SJa_P102	35	H2/O2/N2	29.58%,7.39%,63.03%	0.5	1001.1	2080
22_SJa_P102	36	H2/O2/N2	29.58%,7.39%,63.03%	0.5	1005.4	20,000
22_SJa_P102	37	H2/O2/N2	29.58%,7.39%,63.03%	0.5	999.9	10,000

22_SJa_P102	38	H2/O2/N2	29.58%,7.39%,63.03%	0.5	999.2	5000
22_SJa_P102	39	H2/O2/N2	29.58%,7.39%,63.03%	0.5	1000	5000
22_SJa_P102	40	H2/O2/N2	29.58%,7.39%,63.03%	0.5	997.4	5000
22_SJa_P102	41	H2/O2/N2	29.58%,5.92%,64.50%	0.4	999	5000
22_SJa_P102	42	H2/O2/N2	29.58%,5.92%,64.50%	0.4	999	5000
22_SJa_P102	43	H2/O2/N2	29.58%,5.92%,64.50%	0.4	999	10,000
22_SJa_P102	44	H2/O2/N2	29.58%,5.92%,64.50%	0.4	999	20,000
22_SJa_P102	45	H2/O2/N2	29.58%,5.92%,64.50%	0.4	996.5	20,000
22_SJa_P102	46	H2/O2/N2	25.15%,15.72%,59.13%	1	995	100
22_SJa_P102	47	H2/O2/N2	25.15%,15.72%,59.13%	1	998.1	100
22_SJa_P102	48	H2/O2/N2	25.15%,12.57%,62.28%	0.8	999.8	100
22_SJa_P102	49	H2/O2/N2	25.15%,9.43%,65.42%	0.6	996.8	100
22_SJa_P102	50	H2/O2/N2	25.15%,9.43%,65.42%	0.6	1001.9	330
22_SJa_P102	51	H2/O2/N2	25.15%,7.86%,66.99%	0.5	997.6	330
22_SJa_P102	52	H2/O2/N2	25.15%,6.29%,68.56%	0.4	1001.1	330
22_SJa_P102	53	H2/O2/N2	25.15%,6.29%,68.56%	0.4	1001.1	660
22_SJa_P102	54	H2/O2/N2	25.15%,6.29%,68.56%	0.4	1001.1	1,000
22_SJa_P102	55	H2/O2/N2	25.15%,6.29%,68.56%	0.4	1001.1	1,600
22_SJa_P102	56	H2/O2/N2	25.15%,6.29%,68.56%	0.4	1001.1	5,000
22_SJa_P102	57	H2/O2/N2	25.15%,6.29%,68.56%	0.4	1001.1	20,000
22_SJa_P102	58	H2/O2/N2	25.15%,6.29%,68.56%	0.4	997.2	10,000
22_SJa_P102	59	H2/O2/N2	25.15%,6.29%,68.56%	0.4	997.2	15,000
22_SJa_P102	60	H2/O2/N2	25.15%,6.29%,68.56%	0.4	997.2	20,000
22_SJa_P102	61	H2/O2/N2	25.15%,6.29%,68.56%	0.4	997.2	30,000
22_SJa_P102	62	H2/O2/N2	25.15%,6.29%,68.56%	0.4	1003	10,000
22_SJa_P102	63	H2/O2/N2	25.15%,6.29%,68.56%	0.4	1003	15,000
22_SJa_P102	64	H2/O2/N2	25.15%,6.29%,68.56%	0.4	1003	20,000
22_SJa_P102	65	H2/O2/N2	25.15%,6.29%,68.56%	0.4	1003	30,000
22_SJa_P102	66	H2/O2/N2	25.15%,6.29%,68.56%	0.4	998.5	10,000
22_SJa_P102	67	H2/O2/N2	25.15%,6.29%,68.56%	0.4	998.5	15,000
22_SJa_P102	68	H2/O2/N2	25.15%,6.29%,68.56%	0.4	998.5	20,000
22_SJa_P102	69	H2/O2/N2	25.15%,6.29%,68.56%	0.4	997.7	30,000
22_SJa_P102	70	H2/O2/N2	25.15%,9.43%,65.42%	0.6	996	100
22_SJa_P102	71	H2/O2/N2	25.15%,7.86%,66.99%	0.5	996.2	100

Appendix G – Data Result Sheet

Project	Test Number	lambda [-]	Fuel-Air Equilibrium [-]	Fuel-Oxygen Equilibrium [-]	MIE Cummulative_mJ
22_SJa_P101	1				
22_SJa_P101	2				
22_SJa_P101	3				
22_SJa_P101	4				
22_SJa_P102	1				0.014565461
22_SJa_P102	2				0.037869337
22_SJa_P102	3				0.017706135
22_SJa_P102	4				0.01976297
22_SJa_P102	5				0.022233015
22_SJa_P102	6				0.02286362
22_SJa_P102	7				0.016896056
22_SJa_P102	8				0.025850068
22_SJa_P102	9				0.028931325
22_SJa_P102	10				0.038330344
22_SJa_P102	11	1.00	1.00	1.00	0.013802449
22_SJa_P102	12	1.00	0.99	0.99	0.021548353
22_SJa_P102	13	0.80	0.99	1.24	0.022282503
22_SJa_P102	14	0.60	0.99	1.65	0.025465015
22_SJa_P102	15	0.51	0.99	1.95	0.016475843
22_SJa_P102	16	0.51	0.99	1.95	0.012812824
22_SJa_P102	17	0.51	0.99	1.95	0.014985323
22_SJa_P102	18	0.51	0.99	1.95	0.014624317
22_SJa_P102	19	0.51	0.99	1.95	0.021236215
22_SJa_P102	20	0.51	0.99	1.95	0.01758158
22_SJa_P102	21	0.51	0.99	1.95	0.023615902
22_SJa_P102	22	0.51	0.99	1.95	0.031054309
22_SJa_P102	23	0.51	0.99	1.95	0.025124904
22_SJa_P102	24	0.51	0.99	1.95	0.035272591
22_SJa_P102	25	0.51	0.99	1.95	0.030568769
22_SJa_P102	26	0.51	0.99	1.95	0.027627149
22_SJa_P102	27	0.51	0.99	1.95	0.024061141
22_SJa_P102	28	0.51	0.99	1.95	0.02556932
22_SJa_P102	29	0.51	0.99	1.95	0.035779201
22_SJa_P102	30	0.51	0.99	1.95	0.036798002
22_SJa_P102	31	0.51	0.99	1.95	
22_SJa_P102	32	0.50	1.00	2.00	0.042264221
22_SJa_P102	33	0.50	1.00	2.00	0.04299448
22_SJa_P102	34	0.50	1.00	2.00	0.043623759
22_SJa_P102	35	0.50	1.00	2.00	0.034735678

22_SJa_P102	36	0.50	0.99	1.97	0.188422103
22_SJa_P102	37	0.50	0.99	1.98	0.137676341
22_SJa_P102	38	0.50	1.01	2.01	
22_SJa_P102	39	0.50	1.00	2.01	0.053285434
22_SJa_P102	40	0.50	1.00	2.01	0.065257492
22_SJa_P102	41	0.40	1.00	2.50	0.066409155
22_SJa_P102	42	0.40	1.00	2.50	0.064260536
22_SJa_P102	43	0.40	1.00	2.50	0.102216115
22_SJa_P102	44	0.40	1.00	2.50	0.161994068
22_SJa_P102	45	0.40	1.01	2.51	0.167358611
22_SJa_P102	46	1.00	0.81	0.81	
22_SJa_P102	47	1.00	0.80	0.80	0.016595026
22_SJa_P102	48	0.80	0.82	1.03	0.025507334
22_SJa_P102	49	0.60	0.80	1.34	
22_SJa_P102	50	0.60	0.80	1.33	0.020196018
22_SJa_P102	51	0.50	0.81	1.63	0.032867606
22_SJa_P102	52	0.40	0.80	1.99	0.034338698
22_SJa_P102	53	0.40	0.80	1.99	0.033675839
22_SJa_P102	54	0.40	0.80	1.99	0.02422618
22_SJa_P102	55	0.40	0.80	1.99	0.033544447
22_SJa_P102	56	0.40	0.80	1.99	0.053758896
22_SJa_P102	57	0.40	0.80	1.99	0.170871859
22_SJa_P102	58	0.33	0.80	2.40	0.121313436
22_SJa_P102	59	0.33	0.80	2.40	0.160336365
22_SJa_P102	60	0.33	0.80	2.40	0.188772716
22_SJa_P102	61	0.33	0.80	2.40	0.274685761
22_SJa_P102	62	0.34	0.81	2.39	
22_SJa_P102	63	0.34	0.81	2.39	
22_SJa_P102	64	0.34	0.81	2.39	0.208452666
22_SJa_P102	65	0.34	0.81	2.39	0.299668835
22_SJa_P102	66	0.40	0.79	2.00	0.13414489
22_SJa_P102	67	0.40	0.79	2.00	0.162378271
22_SJa_P102	68	0.40	0.79	2.00	0.19584419
22_SJa_P102	69	0.39	0.80	2.04	0.270125413
22_SJa_P102	70	0.60	0.81	1.36	0.016985535
22_SJa_P102	71	0.50	0.81	1.63	0.020150796